Net fluxes of CO_2 in Amazonia derived from aircraft observations

Wendy W. Chou,[1] Steven C. Wofsy,[1] Robert C. Harriss,[2,3] John C. Lin,[1]
C. Gerbig,[1] and Glenn W. Sachse[2]

Received 15 September 2001; revised 17 April 2002; accepted 18 April 2002; published 16 November 2002.

[1] A conceptual framework is developed using atmospheric measurements from aircraft to determine fluxes of CO_2 from a continental land area. The concepts are applied to measurements of CO_2, O_3, and CO concentrations from the Amazon Boundary Layer Experiment (ABLE-2B, April–May 1987) to estimate fluxes of CO_2 for central and eastern Amazonia late in the wet season of 1987. We observed that column amounts of CO_2 from 0 to 3 km decreased during the day over Amazonia at the average rate of -6.3 ± 1 μmol m^{-2} s^{-1}, corresponding to an uptake flux modestly smaller than the daytime uptake (-10.2 μmol m^{-2} s^{-1}) at a flux tower in the study area. The estimated net flux of CO_2, integrated over 24 hours, was -0.03 ± 0.2 μmol m^{-2} s^{-1}, indicating that the carbon budget of a substantial area of central Amazonia was close to balance in April 1987. We argue that net CO_2 fluxes on the continental scale of Amazonia, with its heterogeneous landscape and large areas of inundation, are strongly modified by the influence of seasonal hydrological factors that enhance respiration and decomposition in forests and wetlands, offsetting growth of forest trees in the wet season. *INDEX TERMS:* 0315 Atmospheric Composition and Structure: Biosphere/atmosphere interactions; 0322 Atmospheric Composition and Structure: Constituent sources and sinks; 1610 Global Change: Atmosphere (0315, 0325); *KEYWORDS:* carbon cycle, Amazon Basin, aircraft measurements

Citation: Chou, W. W., S. C. Wofsy, R. C. Harriss, J. C. Lin, C. Gerbig, and G. W. Sachse, Net fluxes of CO_2 in Amazonia derived from aircraft observations, *J. Geophys. Res.*, *107*(D22), 4614, doi:10.1029/2001JD001295, 2002.

1. Introduction

[2] Global studies of atmospheric CO_2, O_2, and $^{13}CO_2$ indicate that forests have taken up >2 PgC/yr of fossil fuel on average over the last 20 years [*Battle et al.*, 2000]. Inverse models point towards a sink in Northern temperate forests [*Tans et al.*, 1990; *Fan et al.*, 1998; *Ciais et al.*, 1995; *Rayner et al.*, 1999; *Bousquet et al.*, 2000], but forest inventories [e.g., *Houghton et al.*, 1999] suggest much smaller uptake. Alternatively, *Phillips et al.* [1998] and *Malhi and Grace* [2000] proposed that mature Amazonian forests may be major sinks for CO_2, up to 2 Pg C/yr, based on data from ecological plots and eddy correlation flux towers. They cited increasing CO_2 concentrations as a possible stimulus for carbon uptake by tropical forests.

[3] Conflicting claims for carbon sinks are difficult to test due to lack of data over the continents. Most atmospheric CO_2 observations are obtained at surface sites in remote oceanic locations, selected deliberately to minimize the influence of continental sources. Measurements close to sources and sinks are subject to large diurnal and spatial variations, due to daily alternation of uptake and release by vegetation and to variation of surface fluxes over the landscape. Since few data exist over the continents, a priori specifications of flux patterns over the surface play an important role in inverse models [*Kaminski and Heimann*, 2001; *Rayner et al.*, 1999]. Large-scale atmospheric data are needed to evaluate these models and to test inferences from plot-size data indicating uptake of CO_2 by mature tropical forests.

[4] The present paper introduces a new conceptual framework for using concentration data from aircraft to estimate regional fluxes of CO_2 over a continent. We use mass balance calculations for the atmospheric column for each hour of the day, and account for CO_2 from combustion and from long-range transport using CO data. The concepts are applied to historical data acquired in Amazonia during the Amazon Boundary Layer Experiment (ABLE-2B) campaign. Our approach derives values for the rate of daytime uptake by the mosaic of surface vegetation and estimates the regional net 24-hour flux of CO_2. The work extends analysis of column integrals presented for ABLE-2A from 1985 [*Wofsy et al.*, 1988]. The results suggest that the net flux for CO_2 was ~0, averaged over a substantial part of Amazonia, in April 1987 [*Chou*, 1999].

2. Observations

[5] ABLE-2B was conducted in April and May 1987, months 6 and 7 of the 9-month wet season. Instruments on board the NASA Electra aircraft measured CO_2, O_3, CO, NO, aerosols, and meteorological parameters for 21 mis-

[1]Department of Earth and Planetary Sciences, Harvard University, Cambridge, Massachusetts, USA.
[2]NASA Langley Research Center, Hampton, Virginia, USA.
[3]Now at National Center for Atmospheric Research, Boulder, Colorado, USA.

0148-0227/02/2001JD001295

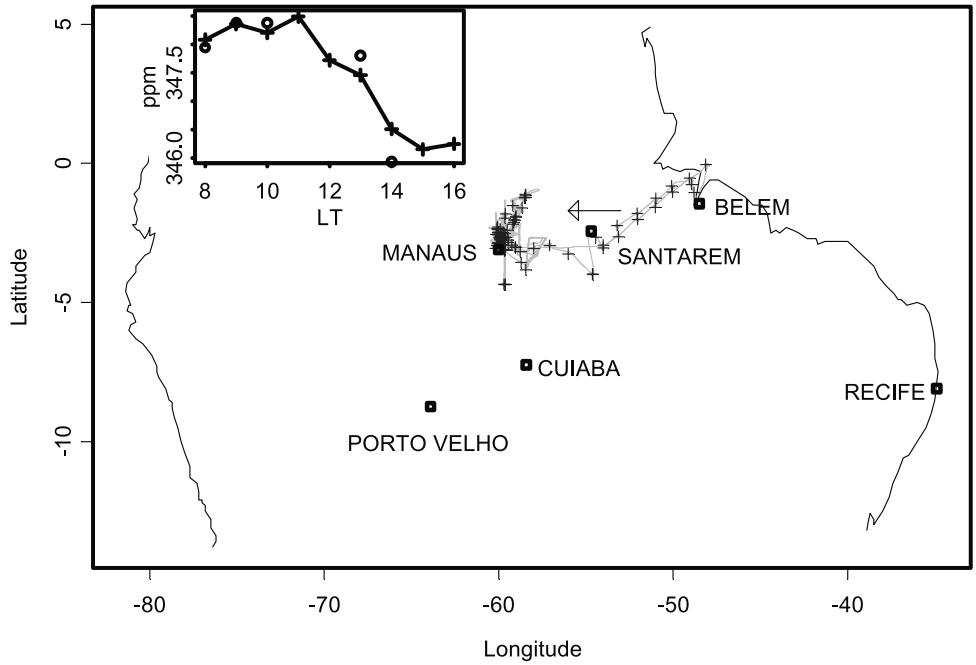

Figure 1. Map showing locations (pluses) for the 85 vertical profiles acquired during ABLE-2B,15 April –8 May 1987.The wind in the lower 3 km of the atmosphere averaged 6.4 m s^{-1} from the East (arrow), giving a transit time of 4.3 days to the main sampling area northeast of Manaus, 2400 km from the ocean. (inset) Diurnal variation of the mean column concentration of CO_2 (0.2–2.8 km) in central Amazonia (pluses, west of −56°) compared to values in eastern Amazonia (circles, east of −56°). See color version of this figure at back of this issue.

sions of four types [*Harriss et al.*, 1990a]: Surveys flew east from Manaus to Belém and back (Figure 1). Source missions intensively sampled the lower atmosphere (0–3 km) over selected vegetation, such as forest or wetland, principally north of Manaus. Convective transport flights covered a wide altitude range to examine the influence of convection. A flux mission obtained eddy-correlation fluxes on level runs in the Planetary Boundary Layer (PBL). A total of 85 vertical profiles were obtained, with dense, repeated coverage in central equatorial Amazonia (1–4 S) and two cross-sections upwind from the main sampling area to the Atlantic coast (Figure 1).

[6] Data for CO_2 were obtained on 15 missions spanning hours from 0700 to 1700 local time (denoted LT, i.e., GMT - 4 hours) over 24 days, at altitudes from 0.15 to ~6 km. Included were: seven source missions (one principally over wetlands) that repeatedly sounded the atmosphere in one area; four transport missions attempting to bound a "volume" and to measure advection and divergence of tracer; three survey missions taking vertical profiles across the Basin; and the flux mission following a racetrack pattern in and just above the Planetary Boundary Layer (see Table 1 and *Chou* [1999]). Most data were acquired between 0.15 and 3.1 km.

Table 1. Electra Aircraft Missions During ABLE 2B

Flight	Local Time	Day of 1987	Mean Latitude, °S	Mean Longitude, °W	Mission Type[a]	Altitude Range, km
6	13–17	105	2.4	60	Transport-double wall	0.3–4.7
7	10–15	107	2.7	60	Transport-volume	0.2–4.6
8	10–14	109	3.8	60	Source	0.2–4.6
9	12–17	110	1.8	59	Source	0.2–4.6
11	8–10	113	2.1	53	Manaus-Belém survey	0.2–3.0
12	7–11	114	NA	51	Belém-Santarém survey	0.2–3.0
13	14–17	114	3.0	58	Santarém-Manaus survey	0.2–3.0
14	7–10	116	2.5	60	Source	0.2–3.0
15	8–9	118	1.2	59	Source	0.2–3.0
16	8–9	119	2.7	59	Source-forest	1.6–4.3
18	11–16	122	3.0	58	Source-wetlands	0.2–4.3
19	11–13	124	2.8	60	Flux	0.8–3.0
20	9–14	126	2.5	60	Transport-volume	0.2–3.7
21	9	127	2.4	60	Source	0.2–4.4
22	11–16	128	2.4	60	Transport-volume	0.2–4.6

[a] *Browell et al.* [1990].

[7] Concentrations of CO_2 were measured using a BINOS non-dispersed infrared analyzer. An upstream Teflon-diaphragm pump drew air from the inlet, into a wet trap at 0°C, to set a constant dew point, then through a pressure-control solenoid valve (MKS capacitance manometer and MKS 250B pressure controller) that maintained the pressure at 740 torr in the wet trap and associated plumbing. A small portion of this flow was drawn into the sample cell by a pump downstream of the analyzer. Constant pressure was maintained in the cell using a second manometer and pressure controller, located downstream of the analyzer and upstream of the pump. Reference gas with near-ambient CO_2 concentration in dry air was passed through the reference cell, maintained at the same pressure as the sample cell. The response time for the instrument to a change in concentration at the inlet was 1–2 s, depending on altitude, corresponding to resolution ~200 m in the horizontal and ~10 m in the vertical.

[8] Calibrations were carried out frequently in flight by flowing standard gases (CO_2 in air, Standard Reference Materials obtained from the National Bureau of Standards) into the inlet, upstream of the wet trap. Calibrations were routinely performed at the beginning, midpoint, and end of each vertical profile to insure unbiased results with respect to altitude. Instrument drift was generally less than ±0.1 ppm during a flight. Calibration gases, stated to be accurate to ±2 ppm, bracketed observed concentrations in the atmosphere. One set of standards was used throughout, insuring uniform measurements during the 24 days of observations.

[9] Corrections were applied to account for BINOS sensitivity to aircraft attitude and acceleration by fitting data from calibrations to a second-order polynomial function of the instantaneous acceleration vector, obtained from a tri-axial linear accelerometer mounted on the instrument. Corrected instrument response had residual sensitivity to rotational accelerations in turbulence and vertical spirals, amounting to a few tenths of 1 ppm, occasionally (in sharp turns) by as much as ±0.5 ppm.

[10] Concentrations of O_3 were measured using ethylene chemiluminescence [*Gregory et al.*, 1990], and concentrations of CO were measured by the Differential Absorption CO Measurement (DACOM) system, a fast-response tunable diode laser spectrometer [*Harriss et al.*, 1990b]. Concentration data, including CO, O_3, and CO_2, were averaged into 10 s intervals and archived. We used archived data to create a merged data set. The instruments did not report concentrations during eddy flux measurements, since accurate calibrations were impossible due to high flow rates.

[11] Additional measurements for CO_2 and O_3 were obtained at a tower in Ducke reserve on the outskirts of Manaus, including eddy covariance fluxes at 41 m and concentrations at 0.02, 3, 6, 12, 27, 36, 41 m [*Fan et al.*, 1990]. Results were reported for ~8 days with mostly non-precipitating conditions. The fetch for this tower was predominantly upland forest without large watercourses or extensive wetlands.

[12] Figures 2a and 2b show data from an illustrative subset of flights. Flight 14 sampled over forests in Central Amazonia northwest of Manaus, flight 12 was a transit flight in eastern Amazonia between Santarém and Belém, and flight 18 measured a mix of wetlands and forests near Manaus. Combustion plumes were observed on flight 14 (note spikes in CO at 7.9, 9.4, and 9.7 hours in Figure 2a), possibly emanating from Manaus. Weaker emissions from biomass fires were seen on many flights. CO_2 data from eastern and central Amazonia were very similar (Figure 1, inset). Figure 2b shows individual profiles, illustrating the reproducibility of the measurements, typically a few tenths of 1 ppm (compare ascent and descent above the PBL, upper panels). Elevated CO_2 is seen at low altitudes in the morning, as CO_2 respired at night mixes upwards into the growing PBL. Low CO_2 just above the morning PBL (0.6–1.2 km) arises from the relict PBL of the previous afternoon, where low CO_2 concentrations (due to photosynthesis) are preserved absent vertical mixing during the night. Small drawdowns were observed consistently in the afternoon, as seen, for example, on flight 18 (Figure 2b, lower panel). Observed differences between CO_2 in the relict PBL and air aloft (≥3 km) were much smaller in Amazonia (3–5 ppm) than in North America in summer (10–20 ppm or more) [*Gerbig et al.*, 2001].

[13] Figures 3a–3c show mean vertical profiles of CO_2, CO and O_3 block averaged by hour and altitude (200 m bins) over the 24 days/15 flights; tower data block-averaged by height and hour of the day were appended at the bottom. The lower atmosphere steadily loses CO_2 during the day due to photosynthetic uptake, although midday CO_2 concentrations remain higher than aloft. Late in the afternoon PBL values were depleted by 1–2 ppm compared to air higher up (Figure 3a). Data for 1400 Local Time are anomalous above ~1.5 km, reflecting unusual CO, O_3 and CO_2 data from a single flight (flight 7), which we judge to be unrepresentative. Apart from these data on flight 7, the flights were remarkably consistent despite fine-scale variance.

[14] The CO_2 profile averaged over the day shows a weak minimum between 1 and 2 km, altitudes where exchange with the surface takes place mainly in the afternoon when concentrations are low. There is a corresponding enhancement of daily mean CO_2 at 500 m and below (Figure 3a). This contrast (''rectification'') arises from the correlated response of photosynthesis and of growth of the PBL to diurnal forcing [*Denning et al.*, 1995, 1999]. The magnitude (~1 ppm) and vertical extent (~2 km) were smaller in ABLE-2B than some model results [*Denning et al.*, 1995]. The density-weighted mean concentration for the whole profile was very close to the value at the top of the profile, notably different from results at midlatitudes [*Gerbig et al.*, 2001], as discussed in detail below.

[15] Concentrations of CO were generally highest near the ground, and typically increased during the day at low altitudes (Figures 3b and 3d), due to inputs from the surface. Concentrations of O_3 were ~20 ppb at 2 km, declined to 10 ppb at the canopy, and vanished at the ground, due to strong uptake by vegetation and weak photochemistry [*Fan et al.*, 1990; *Jacob and Wofsy*, 1990]. Concentrations of O_3 were generally higher at the canopy in the morning than in the afternoon, reflecting maximum uptake (regulated by stomatal opening) by vegetation during daytime.

3. Framework for Analysis of Aircraft Measurements

[16] We wish to derive mass budgets for atmospheric CO_2 and O_3 for the continental region upwind of our observa-

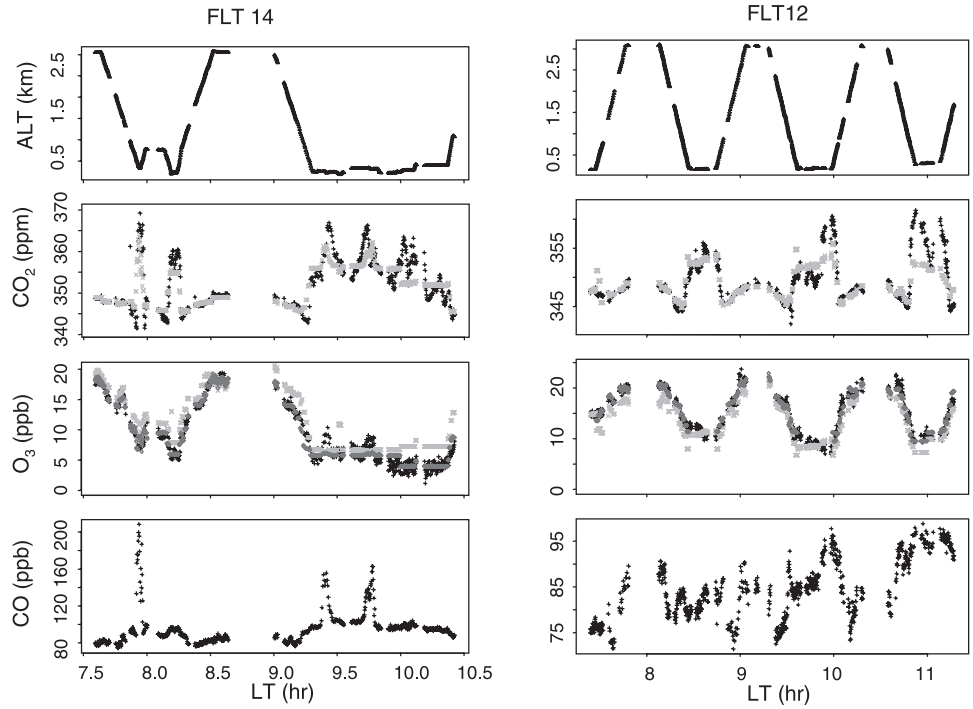

Figure 2a. Data for altitude, CO_2, O, and CO are plotted versus time for flights 12 and 14 (see Table 1). Black points show the observations for 10 s intervals with valid data for CO_2. Blue points show linear model representation of the data using CO as a predictor with hour and altitude as factors. Red points for O_3 add date as a factor to account for variation of background O_3 concentrations. Smoke layers encountered on flight 14 (8, 9.5, 9.7 hours) contributed up to 15 ppm CO_2. See color version of this figure at back of this issue.

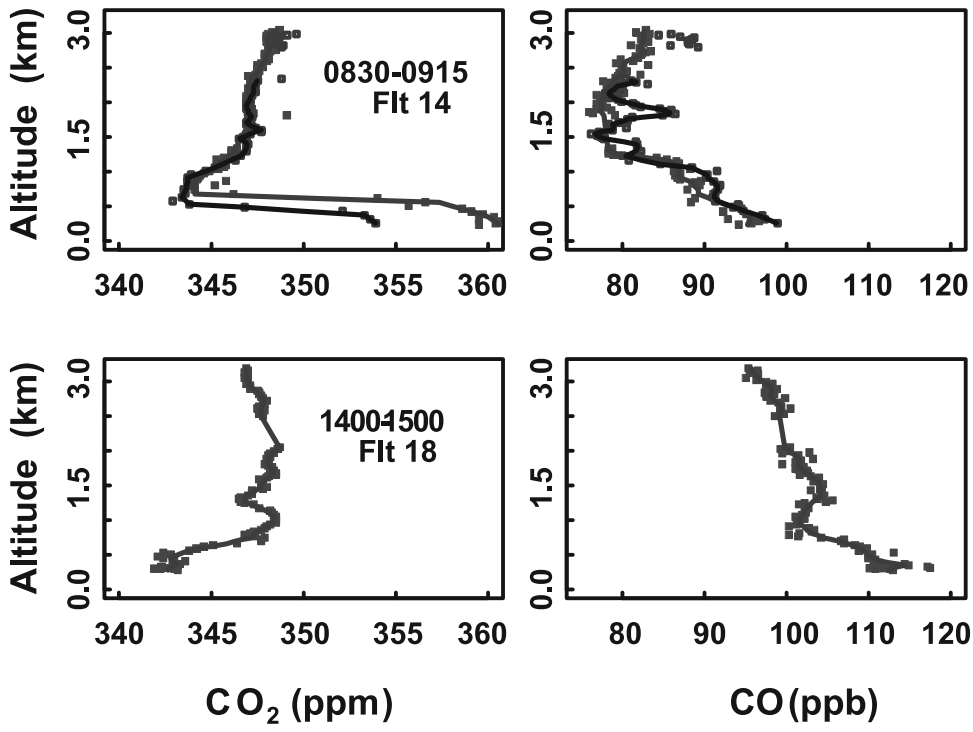

Figure 2b. Vertical profile data (points) for CO_2 and CO for flight 14 (upper panels) and flight 18 (lower panels), and smoothed curves from locally weighted least squares (lines). Note the close agreement of the two profiles (30 minutes apart) above the PBL for both CO_2 and CO in flight 14. Data gaps show locations of midprofile calibrations.

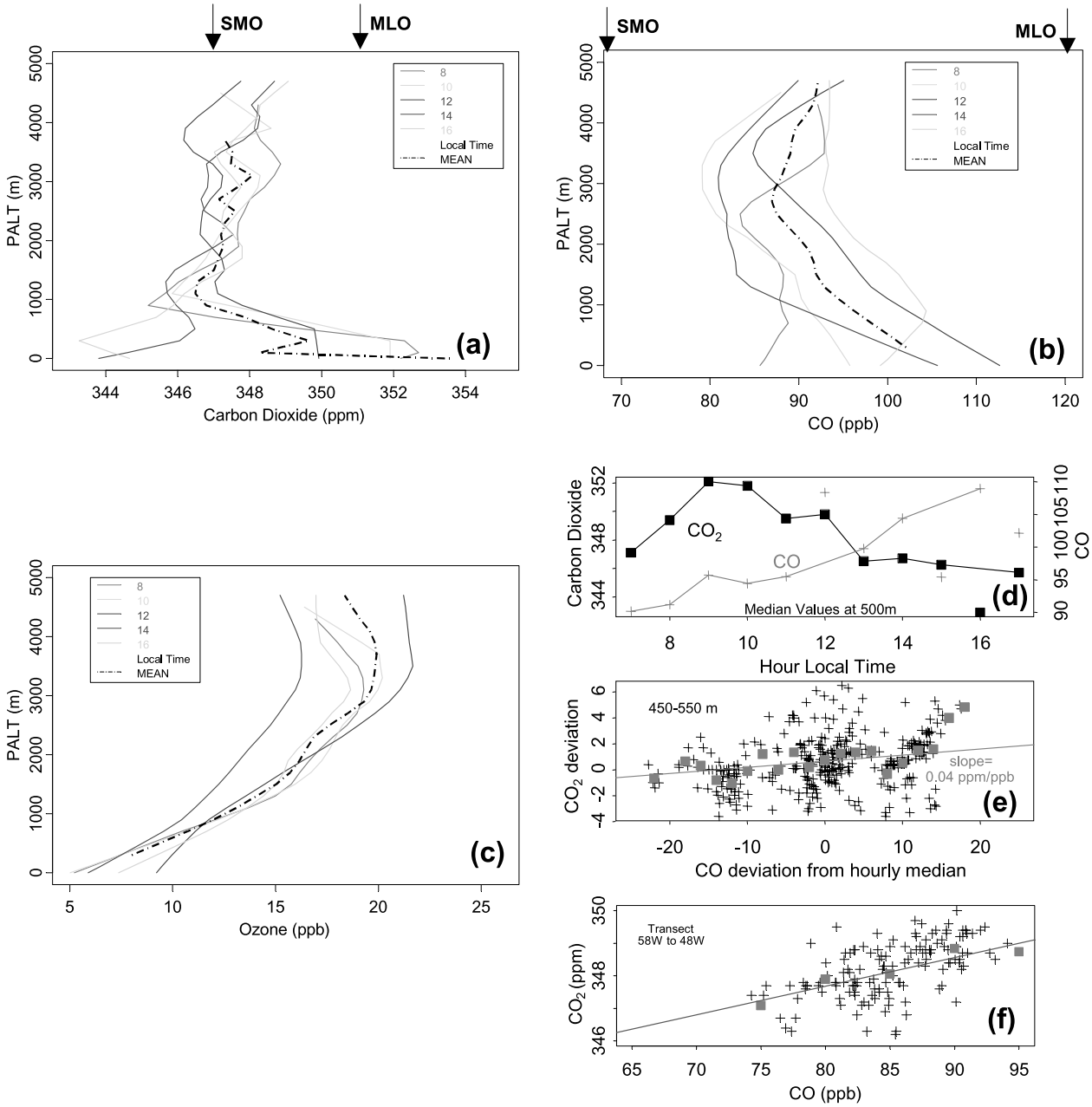

Figure 3. (a) Vertical profiles for CO_2 from 15 flights, days 105–126, 1987, in central Amazonia (Table 1), block averaged by local time. (b) Vertical profiles for CO, as in Figure 3a. Arrows show data from mid-Pacific stations Samoa (SMO, 14° 15′S, 170° 34′W) and Mauna Loa (MLO, 19° 32′N 155° 35′W) for April 1987 (CO_2) and for April 1990 (the first year of station data for CO). (c) Vertical profiles for O_3, as in Figure 3a. (d) Diurnal variation of CO_2 and CO concentrations at 500 m (median values for each hour, all flights). Lines illustrate the general trends during the day. (e) Deviations of CO_2 and CO from the hourly median concentrations (Figure 3d) at 500 ± 50 m. (f) CO and CO_2 gradients across the Amazon Basin (Santarém-Manaus survey) at 3 km altitude: pluses, raw; minuses, block averaged by CO (1 ppb bins, Figure 3e; 5 ppb bins, Figure 3f), linear regression line; straight-line connecting SMO and MLO data points (slope = 0.08 ppm/ppb). See color version of this figure at back of this issue.

tions, from the ground to fixed height *h*. Ideally, we would use a high-resolution mesoscale model to derive rates of mass transport, including detailed representation of convection, but unfortunately this is impossible for our historical data set. Hence we introduce a simple conceptual model representing the basic elements of transport, to elucidate the observational strategies needed to determine continental-scale fluxes from aircraft data. We also examine the influence of fluxes with a diurnally varying component on the near-surface anomalies in tracer concentrations.

[17] Air enters the Amazon Basin with the Trade Winds from the east (Atlantic Ocean) and flows towards a major

region of convergence in western Amazonia. The observed winds were almost due easterly from ~1 to 10 km throughout the equatorial zone, with maximum speed of 10 m s^{-1} at 2 km (see Figure 7a below), turning more northerly right near the surface. Flights in ABLE-2B stayed upwind of the main convergence zone, but mostly downwind of the equatorial forests that lie between Manaus and the ocean [*Santos*, 1987]. Rainfall averaged 200.3 mm during the study [*Garstang et al.*, 1990], ample, but below the long-term mean (~330 mm). Despite significant rainfall, Central and Eastern Amazonia experienced net divergent flow [*Greco et al.*, 1990], providing weak net subsidence (~200 m/day at 700 mb) over the Basin. Convection was limited to small, local storms on 42% of the study days, with moderate-scale, early-morning systems ("basin occurring systems") on 30% of the days. Typical PBL developments, responding to solar heating during the day, were observed over the Basin on these days, accounting for more than 70% of study interval [*Greco et al.*, 1990].

[18] Our simple concept envisions air flowing into the region from the east, with transit time from the sea of 3–5 days. The lower atmosphere accumulates the influence of surface sources and sinks throughout the PBL and associated Convective Cloud Layer (CCL), while exchanging slowly with air from aloft by subsidence (divergence) and intermittent deep convection. Exchange with the surface has the strongest influence for altitudes that interact daily with the ground, namely, up to the maximum daily height, h, of the PBL plus CCL. Thus the chemical composition of air below h is controlled by surface fluxes and by fluxes across h, averaged over a diurnal cycle. In contrast, air above h reflects the large-scale circulation. We select a fixed value for h to include all altitudes in daily contact with the surface, on days with well-defined growth and decay of the PBL, using meteorological and chemical measurements. We considered bounding values (2500 m and 3300 m) to insure that results were not significantly affected by the choice of h.

[19] The concepts are expressed mathematically by vertically averaging the mass continuity equation for tracer in a column with unit area and height h, transported with the mean flow,

$$\mathrm{n_b}\frac{\partial \mathrm{q_{ib}}}{\partial \mathrm{t}}+\frac{\mathrm{n}_h\times(\mathrm{q_{ib}}-\mathrm{q}_{ih})}{\tau_{\mathrm{exch}}}=\left(\frac{\mathrm{S}_i}{h}+[\mathrm{P}_i-\mathrm{L}_i]\right). \qquad (1a)$$

Here S_i denotes surface flux for one of the species for this study, CO_2 or O_3 (mol m^{-2} s^{-1}), $[P_i - L_i]$ is the net chemical tendency averaged over altitudes 0 – h (mol m^{-3} s^{-1}), q_{ib} is the mean mole fraction of tracer i between 0 and h $(q_{ib}\equiv\frac{1}{hn_b}\int_0^h q_i n\,dz)$, $n_b(\equiv\frac{1}{h}\int_0^h n\,dz)$ is the mean atmospheric number density (mol m^{-3}) from 0 to h, n_h is the atmospheric number density at h ($n_{z=h}$), q_{ih} is the mole fraction of tracer at h, and hn_h/τ_{exch} is the mean mass flux of air across h. Time t is measured from the entry of air onto the continent. The "column-averaged net source" (S_i/h + $[P_i - L_i]$) combines the effects of surface flux and chemical reactions on the mean atmospheric composition for altitudes 0 to h. The chemical tendency $[P_i - L_i]$ is zero for CO_2, and negligibly small for O_3 under the conditions for ABLE-2B (see below). The level z = 0 is set at top of the forest canopy, since aircraft data do not resolve CO_2 sources or concentration gradients within the forest.

[20] The main assumption made in equation (1a) is that vertical exchange via cloud venting and subsidence can be represented by a time independent value for τ_{exch}. If vertical exchange through h is not strongly biased towards particular hours of the day, the simple parameterization in equation (1a) does not lead to a bias that can affect inferred values of the net surface source (see Appendix A). The observed pattern of deep convective rainfall in ABLE-2B confirms that q_{ih} may be assumed time-independent. Hence equation (1a) may be rewritten as a differential equation for the difference between q_h and the concentration averaged over the column 0-h, Δq_i ($\equiv q_{ib} - q_{ih}$), in terms of S_i and the mean replacement time for atmospheric mass between 0 and h, $\tau \equiv \tau_{exch}\, n_b/n_h$,

$$\frac{\partial \Delta q_i}{\partial t}+\frac{\Delta q_i}{\tau}=\frac{S_i}{n_b\cdot h}. \qquad (1b)$$

[21] We may divide S_i into a periodic part, S_i' (period T = 1 day, zero mean over 24 hours) plus the 24-hour mean net flux, $\overline{S_i}$ both assumed invariant over the footprint. The solutions Δq_i must likewise have a periodic part, $\Delta q_i'$ with zero mean over 24 hours, and a non-periodic part, $\overline{\Delta q_i}$. Invariance of S_i over the fetch for the flights appears to be an excellent approximation in light of the similarity of average concentrations and diurnal variations in the layer 0-h, from Manaus eastward almost to Belém (Figure 1, inset), as observed in our cross-Basin flights.

[22] Appendix A provides the solutions to equation (1b) for these assumptions. The 24-hour average of Δq_i (defined as

$$\frac{1}{\mathrm{T}}\int_t^{t+\mathrm{T}}\Delta \mathrm{q}_i\,\mathrm{d}t,$$

and denoted by the overbar) is a direct measure of the 24-hour net surface flux (equation (A2)),

$$\overline{\Delta q_i}=\frac{\overline{S_i}\tau}{n_b h}\left(1-e^{-\frac{t}{\tau}}\right), \qquad (1c)$$

where tracer concentrations are assumed well mixed over the ocean ($q_{ib} = q_{ih})_{t=0}$, as observed in ABLE-2A [*Wofsy et al.*, 1988]. Equation (1c) shows that the 24-hour mean column concentration uniformly approaches a steady state that depends only on the 24-hour mean surface flux. The rate of approach depends on the timescale for entrainment from aloft. The 24-hour mean surface flux can thus be determined from the 24-hour mean difference in concentrations between the free troposphere and the lowest layer of the atmosphere (between 0 and h). Periodic (diurnal) changes in concentrations, and associated diurnally varying fluxes, are separable and may be determined independently. These relationships arise from elementary considerations of mass balance, and are more general than the simple derivation given in Appendix A.

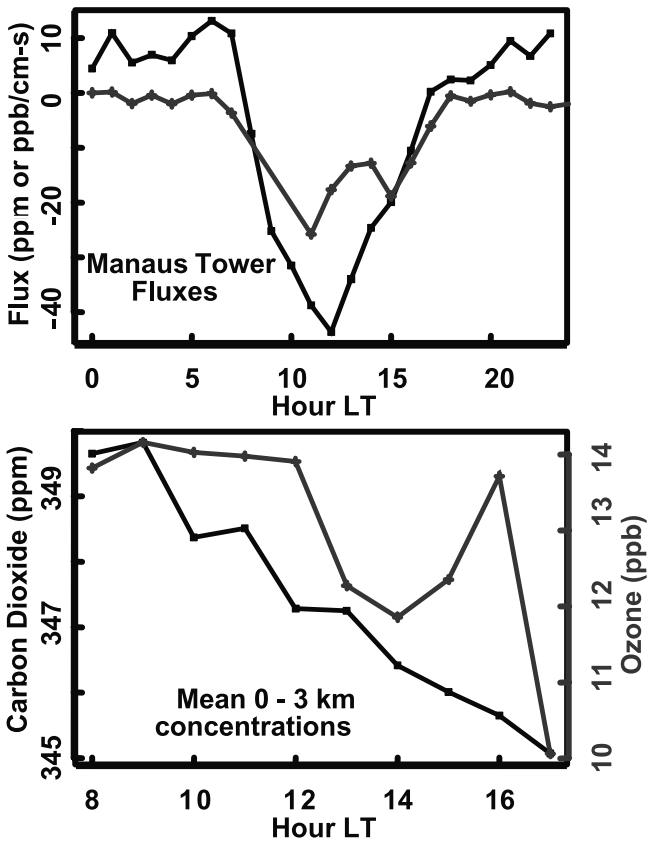

Figure 4. (top) Fluxes of CO_2 (black) and O_3 (gray) versus local time at the Manaus tower [*Fan et al.*, 1990]. (bottom) Density-weighted mean concentrations during the day for the column 0–3.1 km from the aircraft. See color version of this figure at back of this issue.

[23] Equation (1c) implies that there is a similarity relationship for the 24-hour mean concentrations and surface fluxes of two tracers,

$$\frac{\overline{\Delta q_1}}{\overline{\Delta q_2}} = \frac{\overline{S_1}}{\overline{S_2}} \tag{1d}$$

That is, the ratio of vertically integrated net sources for two tracers, averaged over 24 hours, can be derived from the ratio of the differences in concentrations between altitude h (q_h) and the mean from 0 to fixed height h (q_b), $\overline{\Delta q_i}$, also averaged over 24 hours. It is not necessary to know dynamical quantities such as τ. Equation (1d) holds if we sample air parcels with an ensemble of ages, for example due to horizontal dispersion within the Basin, even though equation (1c) would be problematic. The main requirements are separation of diurnal from longer timescales, for both the surface forcing and replacement of PBL air, and linearity of the exchange processes. Equation (1d) is the key relationship we will use to estimate regional fluxes.

[24] In ABLE-2B we obtained data for daytime hours from 7 to 17 hours local time, with a few after 17 hours. The observations confirm that concentrations in the lower atmosphere are quasi-periodic, implying that increases in CO_2 at night must, on average, reverse the daytime drawdown. Our data cover the daily turning points of the column concentrations of CO_2, observed at ~8 hours (daily maxima) and between 16 and 17 hours (minima) in ABLE-2A [*Wofsy et al.*, 1988], when nighttime data were obtained. The turning points are consistent with times for reversal of the CO_2 flux at the tower (Figure 4 [*Fan et al.*, 1990]). Flux reversals occurred when photosynthesis just balanced soil respiration, about 1 hour after sunrise and 1–2 hours before sunset. Thus our daytime data in ABLE-2B are sufficient to derive the 24-hour mean values for q_{ib} required for equation (1d).

[25] The average daytime value of S_i can separately be determined from our hourly data for q_{ib}, including the diurnally varying components of S_i, $\langle S_i \rangle_{\text{day}} = n_b h \langle \partial \Delta q_i / \partial t \rangle_{\text{day}}$ (see Appendix A), where

$$\langle \ldots \rangle_{\text{day}} \equiv \frac{2}{T} \int_{T/4}^{3T/4} \ldots dt$$

is the average value over the daytime hours. These results may be compared to tower data for daytime uptake of CO_2 by the forest [cf. *Wofsy et al.*, 1988].

[26] Our analysis of column budgets using equations (1a)–(1d) differs from the conventional approach that follows concentrations in the Convective Boundary Layer during growth and decay over the day ("CBL method"). In particular, the value of q_{ib} in (1a) is not affected by processes that rearrange concentration gradients between the ground and the fixed level h, e.g., by PBL mixing into the residual layer during the morning.

[27] The height of the fixed level h (Figure 5a) was selected by examining profiles for CO, O_3, and H_2O for each flight to estimate the altitudes influenced by surface exchange, i.e., the height of the PBL plus CCL. The maximum at 1400 local time, 3.1 km, lay at the base of the trade-wind inversion. Analysis of the diurnal variations of CO_2 gave a slightly lower value for the maximum height in daily contact with the surface, 2.5 km. We used both values to analyze data from ABLE-2B.

[28] Since CO_2 is inert in the atmosphere, but ozone is not, similarity requires that the chemical tendency for O_3 ([P − L]) in the atmosphere be small compared to the surface flux S/h. Fluxes of O_3 to the forest were −3.8 and −0.37 nmol m^{-2} s^{-1} in the day and night, respectively (Figure 4, upper panel; *Fan et al.* [1990]), giving $\overline{S_i}/h = -6.8 \times 10^{-13}$ mol m^{-3} s^{-1} for h = 3300 (-8.4×10^{-13} mol m^{-3} s^{-1} for h = 2500 m). Model results [*Jacob and Wofsy*, 1990] indicated that the chemical tendency for O_3 averaged 2×10^{-14} mol m^{-3} s^{-1}, less than 3% of the deposition flux, due to very low concentrations of NO. Hence chemical reactivity was insignificant for O_3.

[29] Fine-scale variations of CO_2 were consistently correlated with concentrations of CO (Figures 2a and 2b), especially in distinct concentration spikes (e.g., Figure 2a, flight 14). Some of this covariance was associated with combustion sources within the study area, but some arose from large-scale (e.g., interhemispheric; Figure 3f) transport. Concentrations of both CO_2 and CO at 3 km and above were bracketed by concurrent values at Samoa (SMO, 14 S) and Mauna Loa (MLO, 19 N), in the mid-Pacific. Changes

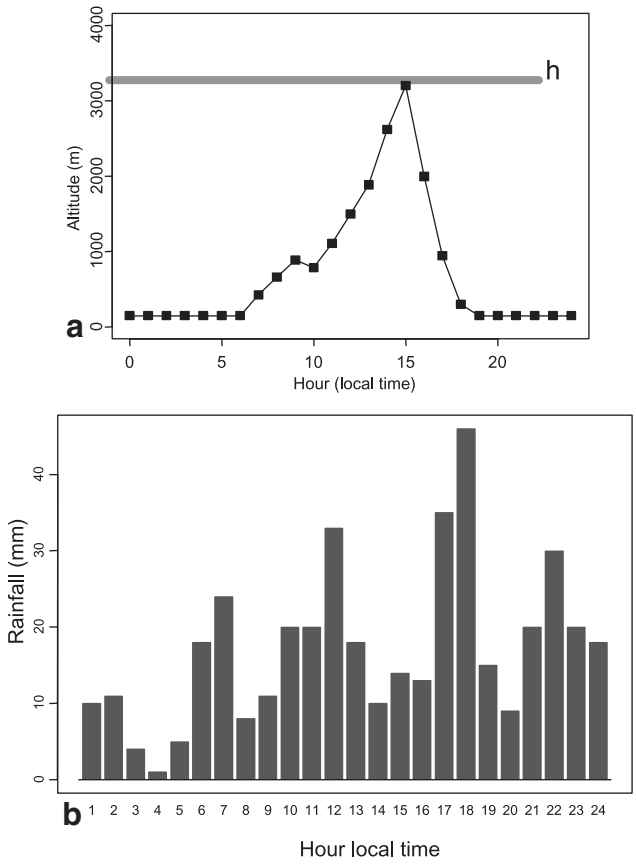

Figure 5. (a) Mean diurnal variation of the height influenced by exchange with the surface inferred from aircraft profiles of CO_2, O_3, H_2O, and temperature. The height h in equation 1 is indicated by the grey horizontal line. (b) Mean hourly rainfall from a basin-wide network of automated weather stations [from *Greco et al.*, 1990].

in CO_2 and CO from W to E across the Amazon Basin closely approximated a mixing line with end-members at SMO and MLO (Figures 3a, 3b, and 3f). These data are consistent with the observation [*Boering et al.*, 1994; *Andrews et al.*, 1999] that concentrations of CO_2 in the upper tropical troposphere may be accurately predicted for any month by averaging data from SMO and MLO, with a delay of 2 months at ~16 km. (Note: Measurements of CO concentrations at MLO and SMO do not exist for 1987. Since seasonal cycles and latitude gradients for CO are reproducible from year to year, we used CO data for 1990, the first available year.)

[30] Our concept requires that we distinguish changes in CO_2 due to forest metabolism from changes due to combustion, or from variable admixtures of Northern and Southern hemisphere air transported into the study area. We observed that combustion and large-scale mixing produced similar correlations, 0.04–0.1 ppm CO_2/ppb CO [cf. *Andreae et al.*, 1988]. We therefore developed a statistical relationship between CO and CO_2 at each altitude to remove the influence of these processes on q_{ib} and q_{ih}. We compared the result to straightforward conditional sampling that removed high CO values, as described below.

[31] A key assumption in the derivation of equation (1d) is that q_h does not change as air transits across the basin from the Atlantic, despite the influence of deep convection. The Cross-Basin survey data supported this view, once the effects of large-scale mixing were removed. Thus it appears that air entrained into the PBL during transit may be assumed to have concentration q_{ih}. Another assumption is that air leaving the column has the 24-hour column mean concentration, q_{ib}. If convection occurred preferentially at times of day when concentrations of CO_2 in the PBL differed from the 24-hour mean value, transport through level h could be biased (see Appendix A). Fortunately the distribution of convective rainfall over the day was almost unbiased relative to the diurnal cycle of CO_2 (Figure 5b), and the bias in $q_{ib} - q_{ih}$ was estimated to be at most 10% towards lower concentrations. Observed precipitation was notably less biased towards afternoon than predicted by some models [e.g., *Peylin et al.*, 1999].

4. Linear Models Representing the Aircraft Data Set

[32] We sought mean profiles representing all 15 flights throughout the Basin for 24 days, to average out variations associated with weather, particular locations, instrument noise, etc., using CO as a tracer to remove the influence of combustion and of long-range advection (interhemispheric exchange). We adopted several alternative approaches to this averaging problem, to insure we did not introduce spurious results.

[33] First we defined mean profiles by block-averaging all data by hour and by altitude (200 m intervals) and then computed column-mean concentrations q_{ib} and concentrations at h (q_{ih}) for each hour of the day. This simple procedure does not account for combustion inputs or long-range transport. Next, we used conditional sampling, removing O_3 and CO_2 data associated with CO values >90 ppb, and block-averaged the remaining data (3400 of 9400 observations) as before. Conditional sampling insures that artifacts due to combustion inputs and large-scale advection are small, but slight biases could remain. Results for these methods were very close (within 0.1–0.2 ppm) to those obtained using the more complete treatment described below, indicating that our procedures to account for systematic covariance of CO and CO_2 did not introduce artifacts.

[34] Our third method derived linear functions to represent data for CO_2 and O_3 in each 200-m altitude band, using three predictors, hour of the day, altitude, and CO, following *Potosnak et al.*, [1999]. We treated hour and altitude as discrete factors and the concentration of CO as a continuous linear predictor, with one coefficient for all hours at each altitude. The equations for the "Linear Model" are

$$[CO_2]_j = a_{j0} + a_{j1}[CO]_j + \Sigma_i\, a_{ji}\, \delta_{ti}, \tag{2a}$$

$$[O_3]_j = b_{j0} + b_{j1}[CO]_j + \Sigma_i\, b_{ji}\, \delta_{ti}. \tag{2b}$$

Here $[CO_2]_j$ and $[CO]_j$ denote observed concentrations in each 10 s interval falling in the jth altitude band at hour t (truncated to the nearest hour). The terms $\sum_i a_{j\,i}\,\delta_{ti}$ or $\sum_i b_{j,i}\,\delta_{ti}$ represent mean concentrations at each altitude in the

Table 2. CO_2 Linear Model[a]

Altitude, m	Mean	σ_r	R^2	a_{j1}
100	349.488	15.1	0.74	0.1891
300	350.704	21.8	0.65	0.0875
500	349.282	17.0	0.51	0.0902
700	348.475	7.03	0.45	0.0701
900	347.315	5.05	0.47	0.0823
1100	346.738	3.04	0.41	0.0667
1300	346.663	2.45	0.33	0.0816
1500	347.107	2.54	0.22	0.0692
1700	347.291	2.14	0.36	0.0871
1900	347.360	1.40	0.24	0.0484
2100	347.340	1.24	0.36	0.0468
2300	347.391	0.98	0.33	0.0371
2500	347.449	1.25	0.23	0.0516
2700	347.190	1.11	0.36	0.0428
2900	347.700	1.46	0.46	0.0732
3100	348.334	1.26	0.34	0.0171
3300	347.325	2.13	0.46	0.1123
3500	347.350	2.83	0.69	0.1569
Mean	347.806	5.00	0.42	0.078

[a] Mean equals 24 hour average (ppm).

(ith) hour (7 to 17, local time), a_{ji} or b_{ji}. Values of coefficients {a} and {b} were optimized using generalized regression for eighteen 200-m altitude bands (Tables 2 and 3), with 10 time-of-day factors for each altitude (the mean for 7 h at altitude j is absorbed into a_{j0} or b_{j0}).

[35] Equation (2) with optimized coefficients provides mean CO_2 and O_3 at each altitude for each hour, and the mean dependence on CO at each altitude. We can then generate synthetic CO_2 profiles, in which the effects of combustion sources and advected CO_2 are removed by setting CO to its background concentration.

[36] If we allow for residual variance from the CO_2 instrument, 1–2 ppm, the Linear Model accounted for more than 60% of observed atmospheric variance up to about 1100 m, excellent fits considering the composite treatment of data spanning a month (see Table 2, and fitted points for typical flights in Figure 2a). Above ~1300 m instrument variance exceeds atmospheric variance and the fits are difficult to assess. The coefficients for CO_2 dependence on CO were consistent throughout the lower part of the profile (200–1700 m), with overall mean value 0.078 ± 0.04 (1σ) ppm/ppb. This value lies within the range observed for biomass burning [*Andreae et al.*, 1988] and large-scale mixing (0.04–0.1).

[37] Residual variance for O_3 increased with altitude as concentrations increased, in contrast to the results for CO_2. Coefficients for CO in the O_3 fits were variable because the dependence of O_3 on CO was weak (Table 3). Ozone varied less than CO_2 with time-of-day but more from flight-to-flight. To test if flight-to-flight variance affected derived values of q_{ib} and q_{ih} for ozone, we constructed another linear model by adding a factor variable for each of the 15 flights. The model produced values of $(O_{3b}-O_{3h})$ very similar to results both from the Linear Model and from conditional sampling, and we concluded that variability in background O_3 did not affect the analysis.

5. Results: Budget of CO_2 Over Amazonia

[38] Figures 6a–6d show profiles for CO_2 and O_3 from the Linear Model, with influences of combustion and large-scale exchange removed by setting the concentration of CO in equation (2) to the estimated CO background concentration, chosen as the 20th percentile for all flights (84 ppb) following *Potosnak et al.* [1999]. Data from the tower were appended at the bottom. Results were insensitive to the choice of percentile corresponding to the background value: the 10th and 30th percentiles gave 80.3 ppb and 87.7 ppb, respectively, corresponding to ±0.3 ppm CO_2 or less.

[39] The Linear Model functions provide smooth vertical profiles for each hour, and smooth diurnal variations for each altitude (excepting 14 hours; see Figures 6a and 6b). Since each altitude and hour was treated independently, the smooth behavior supports the validity of the data averaging. Mean hourly and daily values of q_{ib} and q_{ih} are shown in Figures 6c–6f, derived from profiles in Figures 6a and 6b by averaging from 0–2500 m or 0–3300 m. Tower data for 41 m were adopted for 0–75 m, and values of q_{ib} and q_{ih} at 14 LT were replaced with the mean of 13 and 15 LT as noted above. It appears that CO_2 was added to the column after 17 hours, consistent with the flux data from the Manaus tower (Figure 4) and data from ABLE-2A [*Wofsy et al.*, 1988], but data were too few to give reliable values for q_b at 1700 LT.

[40] We fit smooth curves to the profiles in Figures 6a and 6b and computed residuals, to estimate random errors at each altitude. The estimated uncertainties for CO_2 at each hour and altitude were smaller than ±1 ppm. Uncertainties in mean column concentrations were estimated by fitting straight lines to the data in Figures 6c–6f and computing standard errors of the value at 12 LT; results were smaller than ±0.3 ppm. Corresponding values for O_3 were ±2 ppb and ±0.5 ppb, respectively.

[41] Tables 4a (O_3) and 4b (CO, CO_2) give values for $(q_{ib}-q_{ih})$ averaged over daytime (i.e., between the turning points, 8–17, covering hours 8–16 hours in Figure 6), which we will equate to $\overline{\Delta q_i}$, for three treatments: "all data," block averaged by altitude (no linear model or conditional sampling); Linear Model, equation (2) with no CO adjustment (CO set to the block-averaged mean), presented to show the influence of the CO adjustment; and "Linear Model, CO_{bkgd}," equation (2) with CO set to

Table 3. O_3 Linear Model

Alt. (m)	Mean	σ_r[a]	R^2	b_{j1}
100	9.564	5.74	0.50	0.1378
300	8.246	6.06	0.22	−0.0057
500	9.446	4.86	0.15	−0.0372
700	12.108	8.44	0.41	0.0466
900	11.733	6.02	0.17	0.0359
1100	13.2465	6.93	0.17	0.0725
1300	14.3656	6.35	0.33	0.0589
1500	15.1017	5.77	0.36	0.0776
1700	15.7222	5.73	0.25	0.0672
1900	17.0503	4.98	0.24	0.0754
2100	16.7096	9.73	0.16	0.0645
2300	17.1151	11.8	0.20	0.0901
2500	17.8334	10.3	0.25	0.0505
2700	18.5788	7.71	0.18	−0.0720
2900	18.9267	11.7	0.39	−0.2068
3100	19.1500	16.1	0.37	−0.2535
3300	19.0895	18.8	0.53	−0.2697
3500	19.3832	17.9	0.56	−0.3299
Mean	15.187	9.1	0.30	−0.022

[a] σ_r, square root of the residual variance (ppm for CO_2, ppb for O_3).

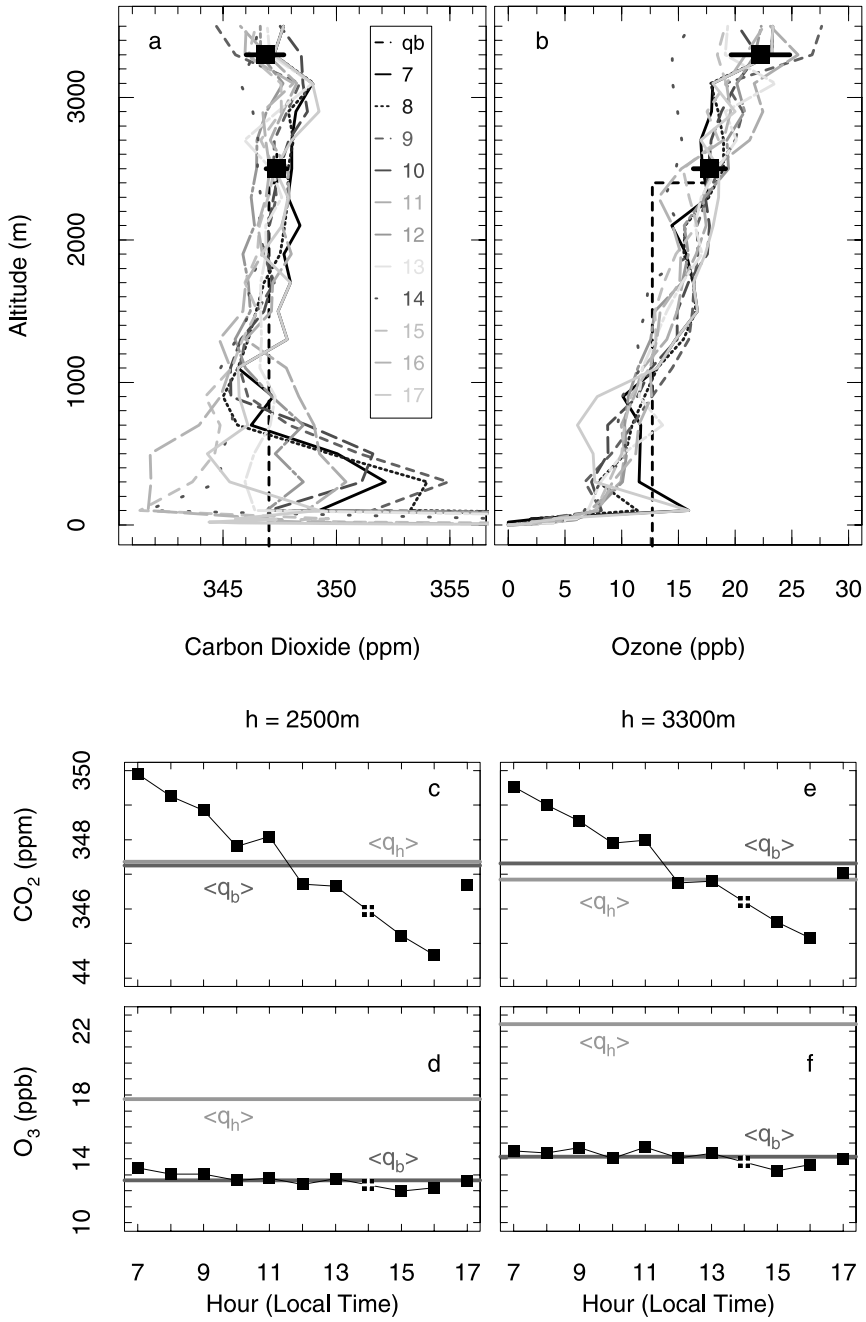

Figure 6. Concentrations for CO_2 and O_3 from Model 1, with CO set to 84 ppb and tower data appended at the bottom: (a) and (b) mean hourly profiles for CO_2 and O_3, respectively; solid squares, daily mean at h = 2.5 and 3.3 km, vertical dashed line, q_b; (c) and (d) for h = 2.5 km: solid squares, hourly column-means for CO_2 and O_3; (light gray, q_b), daily averages for 0-h; (dark gray, q_h), at h; (e) and (f) same as Figures 6c and 6d, for h = 3.3 km. Hour = 14 was interpolated, and hour 17 was excluded from the computation of regional flux. See color version of this figure at back of this issue.

84 ppb. Results for "All Data" and Linear Model with CO_{obs} are similar for both CO_2 and O_3 in most cases, indicating fidelity of the linear functions. The conditional sampling results were very close to the Linear Model with CO_{bkgd}. In almost all cases, using observed CO gives a more positive value for Δq than CO_{bkgd} for both CO_2 and O_3, reflecting combustion-derived CO_2 ($\sim$0.6 ppm) and pollution-derived O_3. These are relatively small corrections.

Table 4a. $\overline{\Delta q_i} \equiv (q_b - q_h)$ Diurnal Mean for Different Data Treatments: ΔO_3[a]

Altitudes (m)	All data	Linear Mdl [COobs]	Linear Mdl [COBkgd]
0–3300	−5.40	−7.73	−8.24
30–2500	−4.48	−4.80	−5.05

[a] Units are ppbv.

Table 4b. $\overline{\Delta q_i} \equiv (q_b - q_h)$ Diurnal Mean for Different Data Treatments: CO_2 and ΔCO_2[a]

Treatment	$q_{h=3300}$	$q_{b\ (0-3300)}$	Δq_{3300}	$q_{h=2500}$	$q_{b\ (0-2500)}$	Δq_{2500}
"All data"	347.80	347.79	*−0.01*	347.45	347.85	*0.40*
Linear $Mdl_{[COobs]}$	346.97	347.80	*0.83*	347.51	347.84	*0.33*
Linear $Mdl_{[COBkgd]}$	346.85	347.10	*0.26*	347.36	347.02	*−0.33*

[a] Units are ppmv. "All data": block averaged data by hour and 200 m altitude intervals (no linear model); "Linear Mdl", equation (2) with CO = block-averaged (time/height) mean; "Linear Mdl, CO_{bkgd}", equation (2) with CO set to background (84 ppb).

[42] Despite the large diurnal variation in the lower part of the profile, results for the daytime average of $((CO_2)_b - (CO_2)_h)$ were surprisingly close to zero for both values of h, 0.6 ± 0.4 ppm without compensating for CO, and -0.03 ± 0.4 ppm when the covariance with CO was removed. The estimated uncertainty for this result accounts for ±0.3 ppm from the central values in Table 4b, plus the uncertainties for the average column amount (see discussion of Figure 6). An additional error of ±0.3 ppm might result from diurnal bias, if our assignments of turning points were off by ±1/2 hour.

[43] The null result for $\overline{\Delta q_i} = 0 \pm 0.7$ ppm for CO_2 (with conservative uncertainty, i.e., adding random and possible bias errors) contrasts markedly with the depletion of O_3 in the column $(0, h)$, -6.4 ± 2.5 ppb (Table 4a). The result also contrasts with CO_2 data over the US in summer [*Gerbig et al.*, 2001], where the atmosphere clearly reflected the activity of surface vegetation. Over well-watered forests, the lower atmosphere was depleted by -5 to -16 ppm CO_2, whereas in drought-impacted areas CO_2 was in excess by 4–10 ppm. The US data support our concept that net sources or sinks of CO_2 should emerge as detectable contrasts between daily-average mean concentrations below h and above h. We conclude from the ∼0 contrast over Amazonia that the CO_2 budget was very close to balance in April 1987.

[44] Without tower data to define CO_2 at the canopy height, we would have computed a value of q_b lower by 0.1–0.2 ppm. This is the effect of the "diurnal rectifier" [*Denning et al.*, 1995], which was smaller than the uncertainty in PBL hourly values. Nevertheless it represents a potential source of systematic bias and should be accounted.

[45] Regional daytime CO_2 uptake at midday, computed from the slope of CO_2 column amounts, was -6.3 μmol m^{-2} s^{-1} for both h = 2500 m and h = 3300 m, slightly lower than daytime fluxes at Manaus (average -10.2 μmol m^{-2} s^{-1} [*Fan et al.*, 1990]). Tower uptake fluxes were ∼30% greater in the morning than the afternoon, due to more cloudiness and stomatal closure in the afternoon. Aircraft data were more symmetrical. The lower uptake rate and greater symmetry for aircraft data may both reflect the influence of wetlands, rivers, and inundated forest, which emit CO_2 at all hours. The tower fetch did not include significant areas of inundation or wetlands.

[46] The net 24-hour biotic exchange fluxes for CO_2 appear to be quite small, -0.13 or $+0.07$ μmol m^{-2} s^{-1} for h = 2500 or 3300 m respectively, using equation (1d) and results for O_3 (taking ΔO_3 from Table 4a, O_3 flux from *Fan et al.* [1990]). Daily mean uptake corresponding to an annual rate of only -0.25 μmol m^{-2} s^{-1} (1 ton C ha^{-1} yr^{-1}) would correspond to ΔCO_2 of -0.8 ppm, at the extreme end of our error bounds for ΔCO_2, with additional allowance for uncertainty in the mean O_3 flux over Amazonia.

[47] Concentrations of CO were lower in ABLE-2B than in ABLE-2A [*Sachse et al.*, 1988]. If we attribute most of the CO enhancements over background to combustion, the associated CO_2 flux from the region was only +0.25 μmol m^{-2} s^{-1} (comparing ΔCO_2 for CO_{obs} versus CO_{bkgd}). These low rates of biomass burning in the wet season nevertheless exceeded regional biogenic uptake.

[48] We estimated the fetch for the aircraft measurements using ozone data combined with rawinsonde measurements, summarized in Figure 7a. Six stations made four soundings daily in and around the Basin. The density-weighted mean wind for 0–3.3 km averaged 6.4 m s^{-1} from the ESE in the main area of aircraft operations (station EMBRAPA), with similar values upwind at Belém and Alta Floresta. The coast is about ∼2400 km ESE of our operational site, giving an average advection time, t_{adv}, of 4.3 days. From the O_3 profiles, which satisfied the quasi-periodic condition, we infer τ_{exch} = 2.7 days from equation (1c) and Table 4a. Pereira [quoted by *Jacob and Wofsy*, 1990] measured ^{222}Rn on the Electra, and inferred $\tau_{exch} \sim$ 3days for the PBL, in harmony with our value. The observation that the advection time exceeds τ_{exch} lends support to the analysis. Likely the true residence time in the Basin, for air in our primary study area, is much longer than t_{adv} due to variance of the wind associated with rain storms, river breeze, inhomogeneous surface heat fluxes, etc. This would further reduce errors associated with our approximate treatment of transport.

[49] The values of t_{adv} and τ_{exch} imply a fetch of roughly 1500 km, extending over the equatorial forest from west of Manaus to southwest of Belém. This is only a rough indication of the area sampled, since wind speed increases with altitude, and mean residence times may be lengthened by dispersive processes. The width of the fetch is probably comparable to the meridional extent of the principal convergence zone in Amazonia, roughly ±500 km. It seems clear that the aircraft observed a vast region of mostly intact equatorial forest and associated mosaics of wetlands, inundated lands (varzea, igapo), as well as the great rivers (20–30% of the land area) at a time of high, and increasing, water levels.

6. Discussion

[50] *Grace et al.* [1996] derived annual mean NEE of -8.5 mol C m^{-2} yr^{-1} (-0.3 μmol m^{-2} s^{-1}) from eddy covariance measurements in Rondônia (10°S, 57°W). *Malhi and Grace* [2000] argued that intact tropical forests globally represent a sink for CO_2 of 2.0 PgC yr^{-1}, stimulated by rising atmospheric CO_2 that could offset 80–90% of the CO_2 source from deforestation. Most of this sink should lie in Amazonia, which has ∼60% of lowland tropical forest globally, and a larger fraction of intact tropical forests. If this mean rate were effective in April 1987 in Amazonia, we should have seen a negative CO_2 gradient close to 1 ppm that was not observed.

[51] Model results (Figure 7b; *Botta and Foley* [2001]) indicate that forest growth should have been near a seasonal

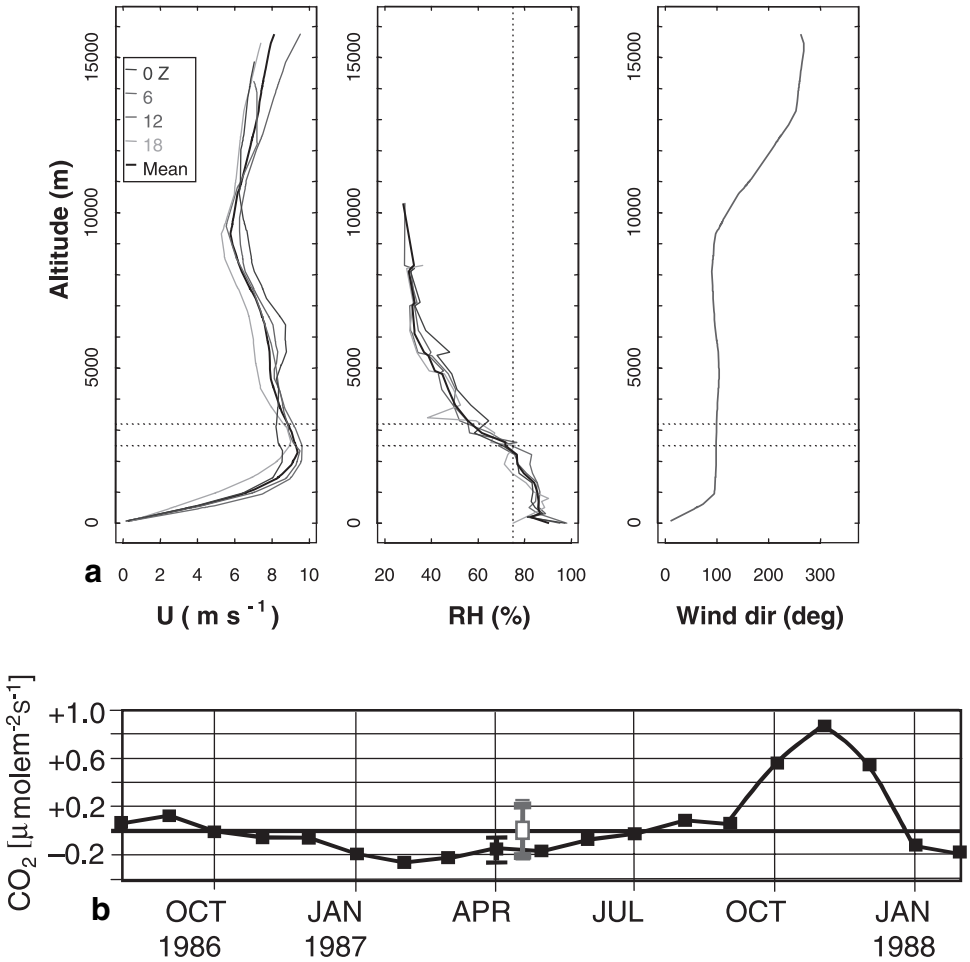

Figure 7. (a) Wind speed (m s^{-1}), relative humidity (%), and wind direction (degrees) at EMBRAPA (60 W, 2.5 S): Averages of four soundings per day (0, 6, 12, 18 GMT, or 20, 2, 8, and 14 local) obtained daily during the experiment [*Cohen et al.*, 1995]; dotted lines show h = 2500 and 3300 m. The sounding data for 5 sites may be retrieved from ftp://ftp-gte.larc.nasa.gov/pub/ABLE2B/GROUND/NOBRE.INPE/. (b) Ecosystem flux for April–May, 1987, computed by the IBIS model (gray symbol) for the study area (58–60W, 1–3S), compared to the regional flux results from ABLE2B (black symbol) (IBIS results courtesy A. Botta and J. Foley, private communication, 2001). Note the ENSO-induced release of carbon in Oct.–Dec. 1987, with strong uptake in the previous wet season (Jan.–May). See color version of this figure at back of this issue.

high in April, 1987. The model computed net exchange of CO_2 for Amazonia from 1935 to 1995, using recorded weather data and the Integrated Biosphere Simulator (IBIS) [*Foley et al.*, 1996; *Kucharik et al.*, 2000] to compute the energy, water, and carbon balances of the land surface, plant physiological processes (photosynthesis, respiration), phenology, plant growth and competition, vegetation dynamics, and nutrient cycling. The uncertainty bars in Figure 7b show the standard deviation of model fluxes for nine $1^\circ \times 1^\circ$ grid squares in the fetch. *Botta and Foley* [2001] found uptake in April–May 1987 slightly greater than the median for April–May in all years, reflecting somewhat sunnier, drier conditions than average. Models indicated release of CO_2 due to drought later in 1987 [cf. *Tian et al.*, 1998], well after ABLE-2B.

[52] Our observations do not show the uptake indicated by the model, although the uncertainty ranges stretch sufficiently to overlap the range of model fluxes in central Amazonia (Figure 7b). Since deforestation and biomass burning are both at seasonal lows late in the wet season, and drought had not yet begun, we expected significant net uptake. Recent tower results from Santarém showed release of CO_2 from an old-growth equatorial forest in the wet season, and uptake in the dry season [*Saleska et al.*, 2001], consistent with the central values from the ABLE-2B aircraft data.

[53] If confirmed, these results would suggest that seasonal variations of respiration may be more important than considered hitherto. Rivers and flooded lands are large, persistent sources of CO_2 to the atmosphere [*Wofsy et al.*, 1988; *Richey et al*, 1990], and a significant quantity of this CO_2 arises from organic matter transported to watercourses from *terra firma* forests and marginal wetlands [*Quay et al.*, 1992]. Tower studies and ecological models generally focus on forests in upland areas, whereas aircraft data integrate over the landscape. Thus we might have expected regional

fluxes to be more positive than fluxes from towers or models. In fact, regional decay rates likely peak late in the wet season, due to hydrological factors not usually modeled: expanding areas of inundation, overland flow of organic matter to water courses, and increased soil moisture. All stimulate decomposition. A plausible explanation for lack of CO_2 uptake in the wet season is that forest growth is masked by seasonal enhancement of decomposition. To test this hypothesis, seasonal variations of both growth and decomposition should be examined, as well as linkages between components of the landscape mosaic.

7. Conclusions

[54] ABLE-2 provided the first comprehensive look at temporal and spatial distributions of CO_2 and other tracers in the tropical atmosphere. We analyzed the historical data for CO_2 in ABLE-2B to show that regional fluxes for CO_2 lead to atmospheric concentration gradients below 3 km that can be quantified by systematic aircraft soundings. A first-order assessment of regional net fluxes for April 1987 was derived by complementing aircraft data with tracer and meteorological data, and with measurements from flux towers. The analysis introduced a framework with (1) "air-mass following" analysis approach; (2) column budgets, instead of conventional CBL budgets; (3) multiple tracers (CO_2, CO, O_3); (4) tracer similarity analyzed by separation of timescales for the surface forcing; and (5) combination of tower data with the above to derive regional fluxes. Future improvements would allow more rigorous application of the column budget approach. Better characterization of fluxes from different vegetation types/ecosystems would be needed, along with application of state-of-the-art mesoscale transport models in place of the simple transport concepts available for ABLE-2B.

[55] Significant covariance was observed between CO_2 and CO, due to the influence of surface sources and large-scale mixing, requiring careful analysis to extract information on regional sources and sinks. The relationship between diurnal variations of CO_2 and convective rainfall was more symmetrical than anticipated, giving rise to only small gradients due to temporal covariance of fluxes and convective overturning ("rectification"). Concentrations of O_3 were strongly depleted in the lower atmosphere due to uptake by the vegetation, a well-characterized process in terms of deposition velocity and flux. Since photochemical rates are very slow in the wet season, net fluxes of CO_2 could be estimated by similarity with O_3.

[56] The layer-mean (0 to h = 3300 m or 2500 m) concentration of CO_2 declined by 3–4 ppm from morning to evening, but the 24-hour average almost exactly equaled the value just above h. We infer that rates for daytime uptake were large, but there was no observable *net* uptake or release of CO_2 over 24 hours. The east-west fetch for these measurements, ~1500 km, encompassed a large fraction of the equatorial Amazon Basin. The lack of regional uptake for CO_2 in the latter stages of the wet season was surprising given the strong ecological reasons to expect net growth of forest trees at this time, and it contrasted sharply with aircraft flights over the northern US in August, 2000.

[57] Our analysis draws attention to a potentially critical difference between studies at ecosystem scales, such as flux towers and ecosystem models, versus regional scales. In Amazonia, up to 30% of the land surface may be inundated late in the wet season, providing strong sources of atmospheric CO_2. Much of the carbon released from these areas is derived from terrestrial sources. Hence the regional CO_2 flux from Amazonia to the global atmosphere may be quite different than the exchange associated with an individual component, even a major component such as *terra firma* forests. Measurements of large-scale landscape mosaics are required in order to determine the carbon budget for a region or continent, and should provide important input for global inverse-model studies. ABLE-2B data provided a preliminary set of large-scale measurements to examine and interpret for these purposes.

Appendix A

[58] We derive a solution to equation (1b) for a case with surface fluxes consisting of two components: (1) a periodic term, S_i', assumed to be invariant in the fetch and to have period 1 day (≡T) and zero mean; and (2) a 24-hour net exchange, approximated as constant in the fetch. Thus $S_i = \overline{S_i} + S_i' = \overline{S_i} + \Sigma_k \mathrm{Re}[S_k \exp(ik\omega t)]$, where $\omega = 2\pi/T$ and T = 24 hours. These assumptions allow us to express Δq_i, the difference between the column-mean concentration of species i between 0 and h and value at q_h, as the sum of a periodic part $\Delta q_i'$ plus a non-periodic part, $\overline{\Delta q_{ib}}$,

$$\Delta q_i = \left(1 - e^{-t/\tau}\right)\overline{S_i}/(n_b h) + \Sigma_k \mathrm{Re}[B_k \exp(ik\omega t)]. \qquad (A1)$$

where

$$B_k = S_k \frac{\tau[1 - ik\omega\tau]}{n_b h\left[1 + [k\omega\tau]^2\right]} = S_k \frac{T}{2\pi k n_b h}\left(-i + \frac{T/\tau}{2\pi k}\right).$$

Here we have assumed that $\Delta q_i = 0$ at the initial time when air enters the Basin, and also that we observe air representing a random ensemble of entry times over 24 hours.

[59] The average value of Δq_i over 24 hours,

$$\frac{1}{T}\int_t^{t+T} \Delta q_i dt \equiv \overline{\Delta q_i}$$

is then given by

$$\overline{\Delta q_i} = \overline{S_i}\frac{\tau^2}{T n_b h}\left(e^{-t/\tau} - e^{-(t+T)/\tau}\right) \approx \overline{S_i}\frac{\tau}{n_b h}\left(1 - e^{-t/\tau}\right), \quad (A2)$$

where the approximation holds for $T/\tau \ll 1$ (i.e., exchange time longer than 1 day). We used the fact that all periodic terms vanish when averaged over 24 hours.

[60] There could be coupling between the diurnally varying transport and the slowly varying part of the column enhancement Δq_i, if the inverse exchange time $1/\tau$ had a periodic variation that correlated with that of $\overline{\Delta q_i}$. Physically this means, that if convection occurred preferentially at times of day when concentrations of CO_2 in the PBL differed from the 24-hour mean value, transport through

level h could be biased and a non-zero value could develop for $\overline{\Delta q_i}$ even if the 24-hour mean surface flux were zero ("rectification"). Fortunately, the distribution of convective rainfall over the day was almost symmetrical relative to the diurnal cycle of CO_2: 45% of rainfall in the Basin occurred between midnight and 1300 LT, when concentrations CO_2 in the lower atmosphere exceed the 24-hour mean, with 55% at times when CO_2 was depleted by photosynthesis in the afternoon (Figure 5b; *Greco et al.* [1990]). Hence deep convection transported air aloft with mean CO_2 very similar to the 24-h mean, with at most a very small bias (10%) towards preferential export of lower concentrations.

[61] The forest takes up CO_2 during the daytime and releases it at night. Our daytime data measures the mass balance of the layer from 0 to h, giving the mean daytime surface flux in terms of the daytime mean of the time derivative of Δq_i

$$\mathrm{RE}\left[\frac{2}{\mathrm{T}}\int_{\mathrm{T}/4}^{3\mathrm{T}/4}\Sigma\frac{S_k}{n_b h}\mathrm{e}^{2\pi\mathrm{ikt}/\mathrm{T}}dt\right]=0,\ \mathrm{k\ even}$$
$$=\mathrm{RE}\left[\Sigma\frac{2}{\pi\mathrm{k}}\frac{S_k}{n_b h}i^{\mathrm{k}-1}\right],\ \mathrm{k\ odd} \tag{A3a}$$

where the integration limits go from sunrise (T/4) to sunset (3T/4). There is a small contribution to the daytime budget associated with non-periodic exchange through altitude h,

$$\mathrm{RE}\left[\frac{2}{\mathrm{T}}\int_{\mathrm{T}/4}^{3\mathrm{T}/4}\Sigma\frac{\partial\Delta q_i}{\partial t}\mathrm{e}^{2\pi\mathrm{ikt}/\mathrm{T}}dt\right]=0,\ \mathrm{k\ even}$$
$$=\mathrm{RE}\left[\Sigma\frac{2}{\pi\mathrm{k}}\frac{S_k}{n_b h}\left(i^{\mathrm{k}-1}+i^{k}\frac{\mathrm{T}/\tau}{2\pi\mathrm{k}}\right)\right],\ \mathrm{k\ odd}. \tag{A3b}$$

Note that the slowly varying exchange term does not contribute at all if S_k is real, i.e., if all source terms change sign at sunrise and sunset: if the system is close to a periodic steady state, Δq_i is higher than the steady-state value in the morning, and exchange with air aloft provides a flux correspondingly higher. However the value of Δq_i and associated exchange fluxes are lower by the same amount in the afternoon, canceling the morning effect and ensuring that flux associated with replacement of the mixed layer has no effect on the 12-hour mean value for Δq_i. Since fluxes of CO_2 from vegetation approximate real, even periodic functions, the value derived for daytime uptake from $\partial\Delta q_i/\partial t$ is insensitive to the slow process of PBL exchange.

[62] **Acknowledgments.** We gratefully acknowledge the contributions of the staff of the Global Tropospheric Experiment and NASA's Langley Research Center and the pilots and crew from the Wallops Flight Facility, who made this work possible. A. D. Botta and J. Foley (University of Wisconsin) generously provided unpublished results from their Amazon model study. This work was supported by grants to Harvard University for airborne CO_2 studies (NASA NAG2-1310) and the Large-Scale Biosphere-Atmosphere study in Brazil (NASA NCC5-341) and by funding for the CO_2 Budget and Rectification Airborne Study (Department of Energy, DOE DE-FG02-98ER62695, the National Science Foundation, NSF ATM-9821044).

References

Andreae, M. O., et al., Biomass burning emissions and associated haze layers over Amazonia, *J. Geophys. Res.*, *93*, 1509–1527, 1988.

Andrews, A. E., K. A. Boering, B. C. Daube, S. C. Wofsy, E. J. Hintsa, E. M. Weinstock, and T. P. Bui, Empirical age spectra for the lower tropical stratosphere from in situ observations of CO_2: Implications for stratospheric transport, *J. Geophys. Res.*, *104*, 26,581–26,595, 1999.

Battle, M., M. L. Bender, P. P. Tans, J. W. C. White, J. T. Ellis, T. Conway, and R. J. Francey, Global carbon sinks and their variability inferred from atmospheric O_2 and $\delta^{13}C$, *Science*, *287*, 2467–2470, 2000.

Boering, K. A., B. C. Daube, S. C. Wofsy, M. Lowenstein, J. R. Podolske, and E. R. Keim, Tracer-tracer relationships and lower stratospheric dynamics: CO_2 and N_2O correlations during SPADE, *Geophys. Res. Lett.*, *21*, 2567–2570, 1994.

Botta, A. D., and J. Foley, IBIS model simulation of monthly CO_2 fluxes for the Amazon and Tocantins Basins: 1935–1998, paper presented at Third LBA-Ecology Science Meeting, Natl, Aeronaut. and Space Admin., Atlanta, Ga., Feb. 2001.

Bousquet, P., P. Peylin, P. Ciais, C. Le Quéré, P. Friedlingstein, and P. P. Tans, Regional changes in carbon dioxide fluxes of land and oceans since 1980, *Science*, *290*, 1334–1336, 2000.

Browell, E. V., G. L. Gregory, R. C. Harriss, and V. W. J. H. Kirchhoff, Ozone and aerosol distributions over the Amazon Basin during the wet season, *J. Geophys. Res.*, *95*, 16,887–16,901, 1990.

Chou, W. W., Estimation of regional net surface fluxes of CO_2 and O_3 over Amazônia from aircraft data, B. A. thesis, Harvard Univ., Cambridge, Mass., 1999.

Ciais, P., P. P. Tans, M. Trolier, J. W. C. White, and R. J. Francey, A large Northern Hemisphere terrestrial CO_2 sink indicated by the $^{13}C/^{12}C$ ratio of atmospheric CO_2, *Science*, *269*, 1098–1102, 1995.

Cohen, J. C. P., M. A. F. S. Dias, and C. A. Nobre, Environmental conditions associated with Amazônian squall lines: A case study, *Mon. Weather Rev.*, *123*(11), 3163–3174, 1995.

Denning, A. S., I. Y. Fung, and D. Randall, Latitudinal gradient of atmospheric CO_2 due to seasonal exchange with land biota, *Nature*, *376*, 240–243, 1995.

Denning, A. S., T. Takahashi, and P. Friedlingstein, Can a strong atmospheric CO_2 rectifier effect be reconciled with a "reasonable" carbon budget?, *Tellus, Ser. B*, *51*, 249–253, 1999.

Fan, S.-M., S. C. Wofsy, P. S. Bakwin, and D. J. Jacob, Atmosphere-biosphere exchange of CO_2 and O_3 in the central Amazon forest, *J. Geophys. Res.*, *95*, 16,851–16,864, 1990.

Fan, S., M. Gloor, J. Mahlman, S. Pacala, J. Sarmiento, T. Takahashi, and P. Tans, A large terrestrial carbon sink in North America implied by atmospheric and oceanic carbon dioxide data and models, *Science*, *282*, 442–446, 1998.

Foley, J. A., I. C. Prentice, N. Ramankutty, S. Levis, D. Pollard, S. Sitch, and A. Haxeltine, An integrated biosphere model of landsurface processes, terrestrial carbon balance, and vegetation dynamics, *Global Biogeochem. Cycles*, *10*(4), 603–628, 1996.

Garstang, M., et al., The Amazon Boundary-Layer Experiment (ABLE 2B): A meteorological perspective, *Bull. Am. Meterol. Soc.*, *71*(1), 19–32, 1990.

Gerbig, C., J. C. Lin, and S. C. Wofsy, Quantification of regional and continental scale surface fluxes of carbon using airborne measurements in a Lagrangian framework, *Eos Trans. AGU*, *82*(20), S83, Spring Meet. Suppl., 2001.

Grace, J., Y. Malhi, J. Lloyd, J. McIntyre, A. C. Miranda, P. Meir, and H. S. Miranda, The use of eddy covariance to infer the net carbon dioxide uptake of Brazilian rain forest, *Global Change Biol.*, *2*, 209–217, 1996.

Greco, S., R. Swap, M. Garstang, S. Ulanski, M. Shipman, R. C. Harriss, R. Talbot, M. O. Andreae, and P. Artaxo, Rainfall and surface kinematic conditions over central Amazonia during ABLE-2B, *J. Geophys. Res.*, *95*, 17,001–17,014, 1990.

Gregory, G. L., E. V. Browell, and L. S. Warren, Amazon basin ozone and aerosol: Wet season observations, *J. Geophys. Res.*, *95*, 16,903–16,912, 1990.

Harriss, R. C., et al., The Amazon Boundary Layer Experiment: Wet season 1987, *J. Geophys. Res.*, *95*, 16,721–16,736, 1990a.

Harriss, R. C., G. W. Sachse, G. F. Hill, L. O. Wade, and G. L. Gregory, Carbon monoxide over the Amazon Basin during the wet season, *J. Geophys. Res.*, *95*, 16,927–16,932, 1990b.

Houghton, R. A., J. L. Hackler, and K. T. Lawrence, The US carbon budget: Contributions from land-use change, *Science*, *285*, 574–578, 1999.

Jacob, D. J., and S. C. Wofsy, Budgets of reactive nitrogen, hydrocarbons, and ozone over the Amazon forest during the wet season, *J. Geophys. Res.*, *95*, 16,737–16,754, 1990.

Kaminski, T., and M. Heimann, Inverse modeling of atmospheric carbon dioxide fluxes, *Science*, *294*, 259, 2001.

Kucharik, C. J., J. A. Foley, C. Delire, V. A. Fisher, M. T. Coe, J. Lenters, C. Young-Molling, N. Ramankutty, J. M. Norman, and S. T. Gower, Testing the performance of a dynamic global ecosystem model: Water

balance, carbon balance and vegetation structure, *Global Biogeochem. Cycl.*, *14*(3), 795–825, 2000.

Malhi, Y., and J. Grace, Tropical forests and atmospheric carbon dioxide, *Trends Ecol. Evol.*, *15*(8), 332–337, 2000.

Peylin, P., P. Ciais, A. S. Denning, P. P. Tans, J. A. Berry, and J. W. C. White, A 3-dimensional study of δO^{18} in atmospheric CO_2: Contribution of different land ecosystems, *Tellus, Ser. B*, *51*, 642–667, 1999.

Phillips, O. L., et al., Changes in the carbon balance of tropical forests: Evidence from long-term plots, *Science*, *282*, 439–442, 1998.

Potosnak, M. J., S. C. Wofsy, A. S. Denning, T. J. Conway, J. W. Munger, and D. H. Barnes, Influence of biotic exchange and combustion sources on atmospheric CO_2 concentrations in New England from observations at a forest flux tower, *J. Geophys. Res.*, *104*, 9561–9569, 1999.

Quay, P. D., D. O. Wilbur, J. E. Richey, J. I. Hedges, A. H. Devol, and R. Victoria, Carbon cycling in the Amazon River: Implications from the C-13 compositions of particles and solutes, *Limnol. Oceanogr.*, *37*, 857–871, 1992.

Rayner, P. J., I. G. Enting, R. J. Francey, and R. Langenfelds, Reconstructing the recent carbon cycle from atmospheric CO_2, delta C-13 and O_2/N_2 observations, *Tellus, Ser. B*, *51*, 213–232, 1999.

Richey, J. E., J. I. Hedges, A. H. Devol, P. D. Quay, R. Victoria, L. Martinelli, and B. R. Forsberg, Biogeochemistry of carbon in the Amazon River, *Limnol. Oceanogr.*, *35*, 352–371, 1990.

Sachse, G. W., R. C. Harriss, J. Fishman, G. F. Hill, and D. R. Cahoon, Carbon-monoxide over the Amazon Basin during the 1985 dry season, *J. Geophys. Res.*, *93*, 1422–1430, 1988.

Saleska, S. R., S. C. Wofsy, B. C. Daube, J. W. Munger, and V. W. Kirchhoff, Carbon balance in the Amazon Basin: Factors influencing the accuracy of eddy covariance measurements., *Eos Trans. AGU*, *82*(47), Fall Meet. Suppl., F221, 2001.

Santos, J., Climate, natural vegetation and soils in Amazônia: An overview, in *The Geophysiology of Amazonia: Vegetation and Climate Interactions*, edited by R. Dickinson, pp. 25–36, Wiley-Interscience, New York, 1987.

Tans, P. P., I. Y. Fung, and T. Takashi, Observational constraints on the global atmospheric CO_2 budget, *Science*, *247*, 1431–1438, 1990.

Tian, H. Q., J. M. Melillo, D. W. Kicklighter, A. D. McGuire, J. V. K. Helfrich, B. Moore, and C. J. Vorosmarty, Effect of interannual climate variability on carbon storage in Amazonian ecosystems, *Nature*, *396*, 664–667, 1998.

Wofsy, S. C., R. C. Harriss, and W. A. Kaplan, Carbon dioxide in the atmosphere over the Amazon Basin, *J. Geophys. Res.*, *93*, 1377–1387, 1988.

W. W. Chou, C. Gerbig, J. C. Lin, and S. C. Wofsy, Department of Earth and Planetary Sciences, Harvard University, 29 Oxford Street, Cambridge, MA 02138, USA. (scw@io.harvard.edu)

R. C. Harriss, NCAR/ESIG, P. O. Box 3000, Boulder, CO 80307-3000, USA. (harriss@ucar.edu)

G. W. Sachse, NASA Langley Research Center, Mail Stop 472, 5 North Dryden Street, Hampton, VA 23681-2199, USA. (g.w.sachse@larc.nasa.gov)

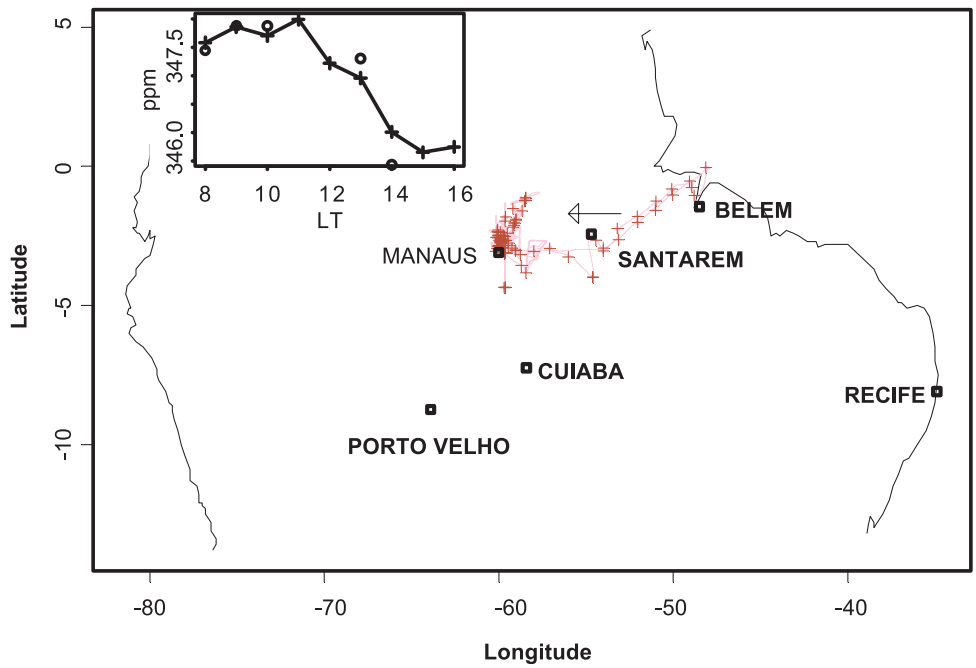

Figure 1. Map showing locations (pluses) for the 85 vertical profiles acquired during ABLE-2B,15 April –8 May 1987.The wind in the lower 3 km of the atmosphere averaged 6.4 m s^{-1} from the East (arrow), giving a transit time of 4.3 days to the main sampling area northeast of Manaus, 2400 km from the ocean. (inset) Diurnal variation of the mean column concentration of CO_2 (0.2–2.8 km) in central Amazonia (pluses, west of −56°) compared to values in eastern Amazonia (circles, east of −56°).

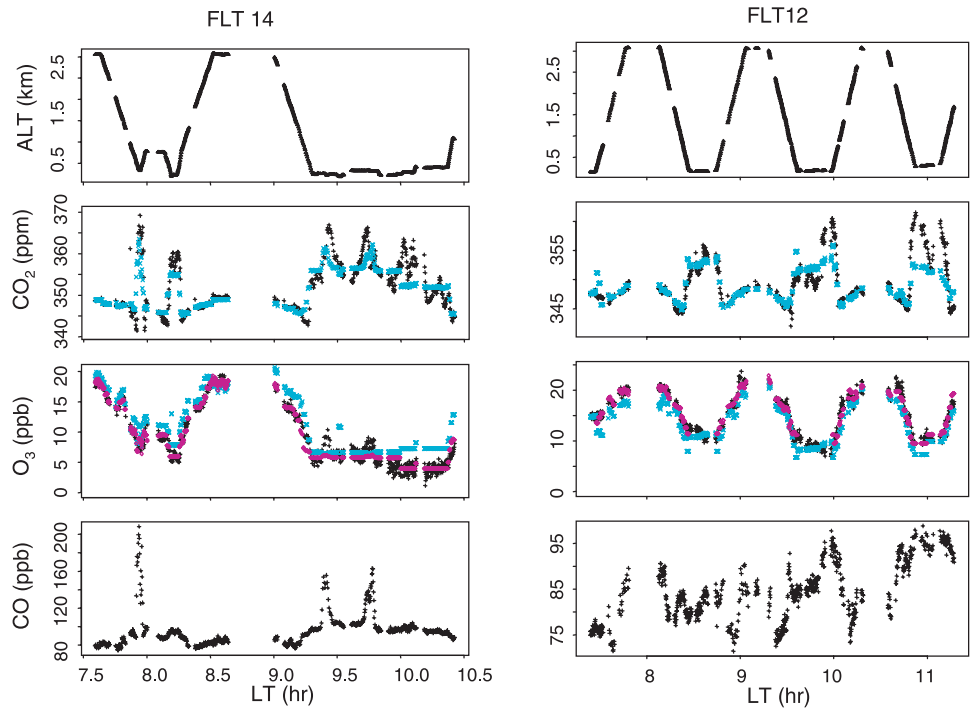

Figure 2a. Data for altitude, CO_2, O, and CO are plotted versus time for flights 12 and 14 (see Table 1). Black points show the observations for 10 s intervals with valid data for CO_2. Blue points show linear model representation of the data using CO as a predictor with hour and altitude as factors. Red points for O_3 add date as a factor to account for variation of background O_3 concentrations. Smoke layers encountered on flight 14 (8, 9.5, 9.7 hours) contributed up to 15 ppm CO_2.

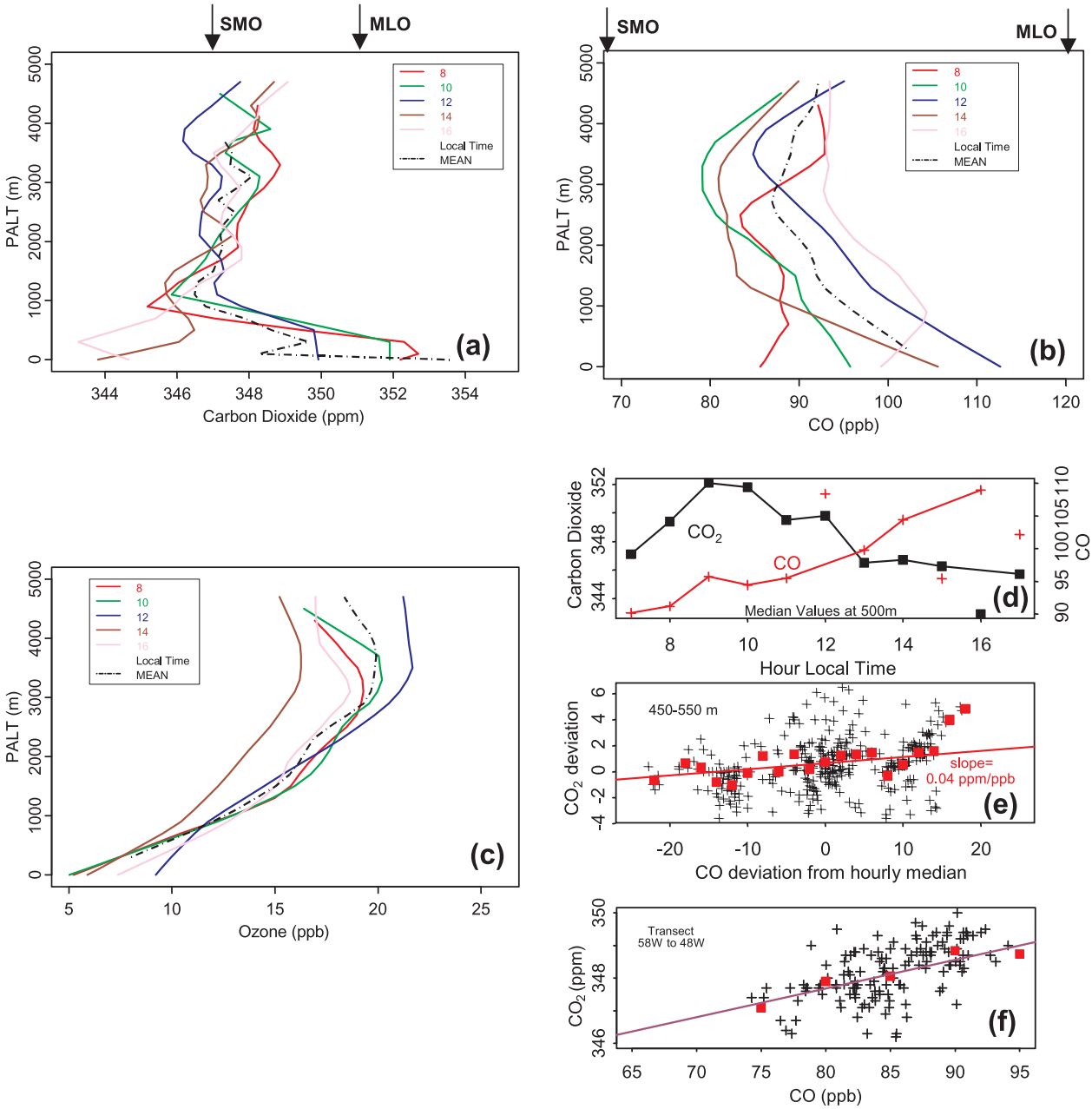

Figure 3. (a) Vertical profiles for CO_2 from 15 flights, days 105–126, 1987, in central Amazonia (Table 1), block averaged by local time. (b) Vertical profiles for CO, as in Figure 3a. Arrows show data from mid-Pacific stations Samoa (SMO, 14° 15′S, 170° 34′W) and Mauna Loa (MLO, 19° 32′N 155° 35′W) for April 1987 (CO_2) and for April 1990 (the first year of station data for CO). (c) Vertical profiles for O_3, as in Figure 3a. (d) Diurnal variation of CO_2 and CO concentrations at 500 m (median values for each hour, all flights). Lines illustrate the general trends during the day. (e) Deviations of CO_2 and CO from the hourly median concentrations (Figure 3d) at 500 ± 50 m. (f) CO and CO_2 gradients across the Amazon Basin (Santarém-Manaus survey) at 3 km altitude: pluses, raw; minuses, block averaged by CO (1 ppb bins, Figure 3e; 5 ppb bins, Figure 3f), linear regression line; straight-line connecting SMO and MLO data points (slope = 0.08 ppm/ppb).

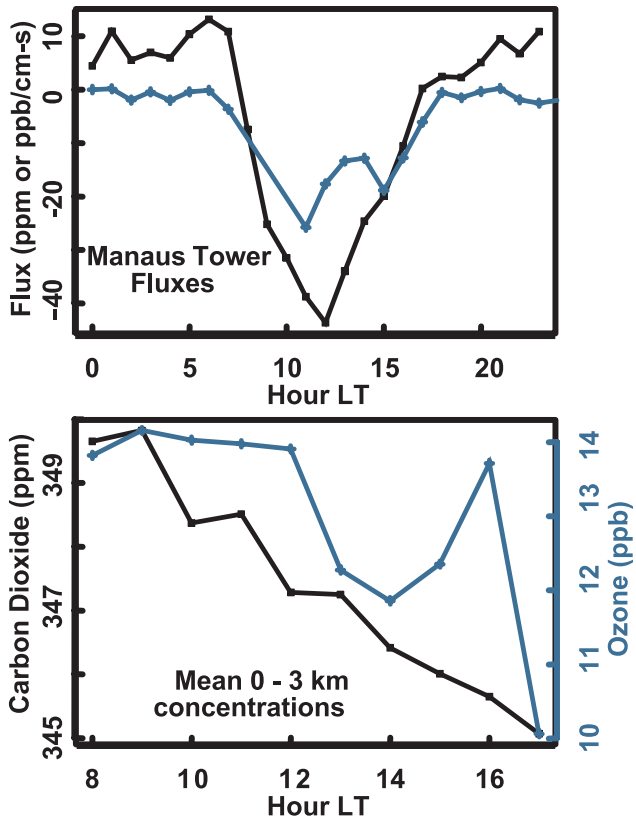

Figure 4. (top) Fluxes of CO_2 (black) and O_3 (gray) versus local time at the Manaus tower [*Fan et al.*,1990]. (bottom) Density-weighted mean concentrations during the day for the column 0–3.1 km from the aircraft.

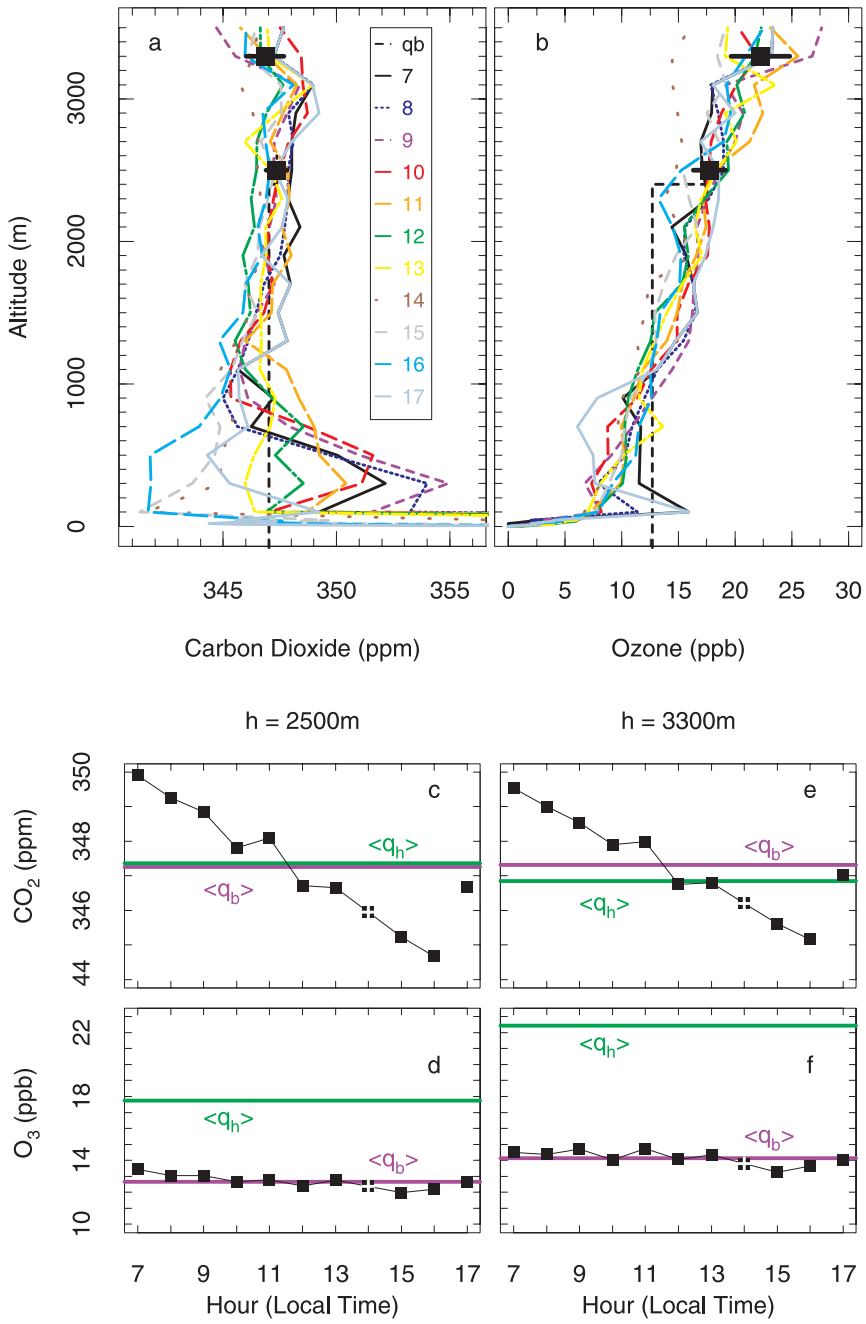

Figure 6. Concentrations for CO_2 and O_3 from Model 1, with CO set to 84 ppb and tower data appended at the bottom: (a) and (b) mean hourly profiles for CO_2 and O_3, respectively; solid squares, daily mean at h = 2.5 and 3.3 km, vertical dashed line, q_b; (c) and (d) for h = 2.5 km: solid squares, hourly column-means for CO_2 and O_3; (light gray, q_b), daily averages for 0-h; (dark gray, q_h), at h; (e) and (f) same as Figures 6c and 6d, for h = 3.3 km. Hour = 14 was interpolated, and hour 17 was excluded from the computation of regional flux.

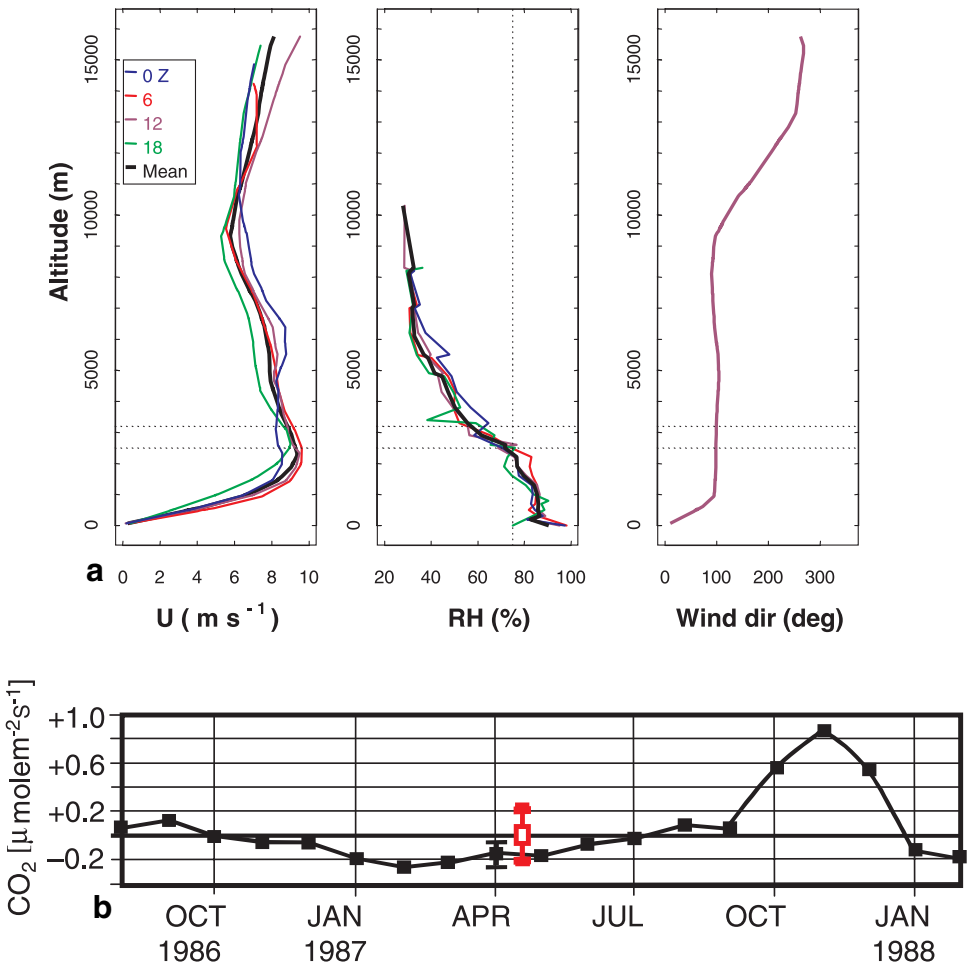

Figure 7. (a) Wind speed (m s^{-1}), relative humidity (%), and wind direction (degrees) at EMBRAPA (60 W, 2.5 S): Averages of four soundings per day (0, 6, 12, 18 GMT, or 20, 2, 8, and 14 local) obtained daily during the experiment [*Cohen et al.*, 1995]; dotted lines show h = 2500 and 3300 m. The sounding data for 5 sites may be retrieved from ftp://ftp-gte.larc.nasa.gov/pub/ABLE2B/GROUND/NOBRE.INPE/. (b) Ecosystem flux for April–May, 1987, computed by the IBIS model (gray symbol) for the study area (58–60W, 1–3S), compared to the regional flux results from ABLE2B (black symbol) (IBIS results courtesy A. Botta and J. Foley, private communication, 2001). Note the ENSO-induced release of carbon in Oct.–Dec. 1987, with strong uptake in the previous wet season (Jan.–May).